Oceanologia, 67 (1)/2025, 67109

https://doi.org/10.5697/TQCH9343

Carbonaceous aerosol particle sources in Manila North Port and the urban environment

Touqeer Gill[1], Simonas Kecorius[1,2,*], Kamilė Kandrotaitė[1], Vadimas Dudoitis[1], Leizel Madueño[3], Alfred Wiedensohler[3], Laurent Poulain[3], Edgar A. Vallar[4], Maria Cecilia D. Galvez[4], Steigvilė Byčenkienė[1], Kristina Plauškaitė[1]

Abstract

This study addresses the pressing issue of black carbon (BC) pollution in urban areas, focusing on two locations in the Philippines: Quezon City's East Avenue (QCG, roadside urban environment) and Manila's North Port. We found that organic aerosol particles (OA) made a greater contribution (80%) to total submicron particulate matter compared to inorganic aerosol (IA) (20%). The mean hourly average equivalent black carbon (eBC) mass concentration at the QCG site (35.97 ± 16.20 $\mu g/m^3$) was noticeably higher compared to the Port (10.27 ± 5.99 $\mu g/m^3$), consistent with trends in other Asian cities. Source apportionment analysis identified eBC related to transport emissions (eBC_{TR}) as the predominant contributor to eBC, accounting for 86% at the Port and 80% at QCG. Diurnal patterns showed the highest eBC_{TR} mass concentrations (47.69 ± 9.34 $\mu g/m^3$) during morning rush hours, which can be linked to light-duty vehicles. Late-night (10 pm–12 am) high concentrations (30.63 ± 8.45 $\mu g/m^3$) can be associated with heavy diesel trucks at the QCG site. Whereas at the Port site, hourly average higher eBC_{TR} concentration (12.24 ± 3.65 $\mu g/m^3$) during morning hours (6 am–8 am) can be attributed to the traffic of heavy-duty trucks, trollers, diesel-powered cranes and ships. Compared to the QCG site, a lower eBC concentration at the Port site was favoured by the more open environment and higher wind speed, facilitating better pollutant dispersion. The mean hourly average concentrations of $PM_{2.5}$ and PM_{10}, measured using an Aerodynamic Particle Sizer, consistently exceeded the air quality standards set by the World Health Organization and the Philippine Clean Air Act at both sites. This study highlights the persisting BC pollution in developing regions and calls for scientifically based strategies to mitigate the air quality crisis.

Keywords

Equivalent black carbon; Source apportionment; Absorption Ångström exponent; Urban environment; Air pollution

[1] *Center for Physical Sciences and Technology (FTMC), Saulėtekio av. 3, LT-10257 Vilnius, Lithuania*
[2] *Institute of Epidemiology, Helmholtz Zentrum München, Ingolstädter Landstr. 1, 85764 Neuherberg, Germany*
[3] *Leibniz-Institute for Tropospheric Research, Permoserstrasse 15, 04318 Leipzig, Germany*
[4] *ARCHERS, CENSER, De La Salle University, 2401 Taft Ave., Malate, Philippines*
***Correspondence**: simonas.kecorius@ftmc.lt (S. Kecorius)

Received: 29 July 2024; **revised:** 23 October 2024; **accepted**: 16 December 2024

1. Introduction

Air pollution is a major environmental issue affecting millions of people worldwide, especially in underdeveloped nations where excessive pollution can cause serious health problems. According to estimates, air pollution-related diseases and deaths impacted more than 6.7 million people worldwide in 2019 (Donaldson et al., 2020). Prolonged exposure to air pollutants has been linked to respiratory and cardiovascular diseases leading to substantial rates of illness and premature death (WHO, 2021). Moreover, air pollution also negatively affects ecosystems, and water bodies and contributes to climate change (Lelieveld et al., 2019). This global crisis presents itself differently in various locations, each facing its difficulties and consequences. In the Philippines, for instance, rapid urbanisation and industrial growth have worsened the issue of air pollution, turning it into a critical concern for public health. According to the World Health Organization (WHO, 2021), outdoor air pollution in the Philippines is responsible for 27,000 premature deaths per year, placing it among the top 20 countries with the highest number of air pollution-related deaths (Myllyvirta et al., 2020). Specific health issues for example asthma, chronic bronchitis, lung cancer, and cardiovascular diseases like heart attacks and strokes have shown significant correlations with days of high air

pollution in the Philippines (Lu et al., 2022). Reports from the Philippine Heart Association (2018) have indicated a marked increase in hospital admissions for heart disease during such periods, highlighting the direct impact of air quality on public health (Yu et al., 2023).

The complete picture of air quality requires investigation of various pollutant metrics, among which particulate matter is a critical component. $PM_{2.5}$ and PM_{10}, particles with aerodynamic diameters less than 2.5 and 10 μm respectively, originate from sources like dust, industrial emissions, and combustion. These particles are key contributors to urban air pollution, affecting both health and climate (Cohen et al., 2017). Delving further, non-refractory PM_1 (NR-PM_1) refers to particles smaller than 1 μm, analysed primarily using advanced aerosol mass spectrometry to understand atmospheric chemistry and its broader impacts (Zuo et al., 2023). Moreover, equivalent black carbon (eBC) is particularly relevant for assessing combustion sources, such as vehicles and biomass burning (Alfoldy et al., 2023).

In developing regions, such as the megacity of Metro Manila in the Philippines, the confluence of rapid urban expansion, deficient infrastructure, and limited resources gives rise to specific concerns regarding air pollution. Metro Manila, housing a population of 12 million and boasting a population density of 21 thousand individuals per square kilometre, faces unique challenges (Philippine Statistics Authority, 2022). Notably, it records the highest number of registered motor vehicles in comparison to other cities in the country, with a reported figure of 2.2 million (Philippine Land Transportation Office, 2023). Given these statistics, it comes as no surprise that a staggering 90% of emissions in this city originate from mobile sources (Environmental Management Bureau, 2018). According to Oanh et al. (2006) the distinctive geographical features of Metro Manila, nestled between Manila Bay to the west and Laguna Lake to the east, result in air quality primarily originating from urban sources, with minimal influence from long-range transported aerosols. In response to air quality issues, the Philippines enacted the Clean Air Act in 1999 and updated it in 2016. This law sets daily and annual limits for PM_{10} (150 $\mu g/m^3$ and 60 $\mu g/m^3$) and $PM_{2.5}$ (50 $\mu g/m^3$ and 25 $\mu g/m^3$) (Republic of Philippines, 1999). It is clear that the air pollution problem in Manila has generated enough momentum to set the right course at the legislative level, but these rules have not been executed thoroughly. As of today, a regulatory agency has not implemented continuous air quality monitoring of major pollutants in Manilla.

Over the years, Manila has been a focal point of numerous studies dedicated to assessing air quality and its associated impact. These research endeavours have furnished invaluable insights into pollutant levels, their diverse sources, and the resultant health risks (Braun et al., 2020). For example, a study by Oanh et al. (2006) investigated the sources of PM in Manila, Philippines. The authors used a chemical mass balance model to estimate the contribution of different sources to PM, including carbonaceous aerosol particles. The results showed that vehicular emissions were the primary source of carbonaceous aerosol particles, followed by biomass burning and coal combustion. Pabroa et al. (2022) analyzed the levels of different air contaminants in Manila, such as particulate matter ($PM_{2.5}$ and PM_{10}), sulphur dioxide (SO_2), nitrogen oxides (NOx), and volatile organic compounds (VOCs) in the city's ambient air. Kecorius et al. (2017, 2019) and Alas et al. (2018) have reported extremely high eBC mass concentrations in Metro Manila, which seem to be a fingerprint of a developing urban environment. These findings provide a baseline for comparison with the current results, which continue to show elevated levels of eBC consistent with rapid urbanisation. Currently, applicable air quality standards for criteria pollutants (e.g. particulate matter) do not include eBC. Focusing solely on PM_{10} or $PM_{2.5}$ may not give adequate information on the state of air quality in Metro Manila, and potentially other megacities. In the study of Madueño et al. (2019) and Kecorius et al. (2017), the aerosol particles were extensively characterized in terms of their particle number size distribution, particle and equivalent black carbon number and mass concentration, mixing state, spatial and temporal pollutant variability, and fleet segregated emission factors. Despite commendable progress in previous investigations, some knowledge gaps remain. For example, little information exists about other BC sources besides road traffic. It is also unclear what influence Manila Port has on eBC levels in the city. While exploring the port area, it is important to understand the potential influence on air quality, particularly regarding port emissions. It is known that port emissions contribute significantly to elevated atmospheric pollutants in the vicinity of the port (Merico et al., 2019; Madueño et al., 2022).

To improve the knowledge about aerosol composition in Metro Manila, this study aims to (1) conduct source apportionment of BC at key sites (Port and QCG), (2) investigate the temporal variability of air pollutants, and (3) analyse the organic and inorganic aerosol composition at Port site. This study supports previous studies and provides further compelling evidence that an outdated vehicular fleet is the primary contributor to the elevated levels of black carbon concentration in Metro Manila. It underscores the urgent need for targeted mitigation strategies to reduce emissions from the transportation sector at both sites.

2. Methods

2.1 Description of measurement site

An intensive field campaign focusing on the physical-chemical properties of the airborne pollutants was conducted at two locations in Metro Manila, Philippines: Manila's North Port (14°61′N, 120°96′E) between December 20,

Figure 1. Map of Metro Manila with the approximate locations of the measurement sites, Manila North Port Harbour, Manila City (a) and East Avenue Quezon City (b).

2019, to January 25, 2020, and Quezon City's East Avenue roadside (14°67′N, 121°04′E) between January 29, 2020, to February 26, 2020. The measurements were carried out as a part of the project "A Transdisciplinary Approach to Mitigate Emissions of Black Carbon" (TAME-BC). The Port site is located 12 km away from the Quezon City's East Avenue (Figure 1). Measurement instrumentation was held in a specialized, air-conditioned measurement container to ensure the quality of data collected; aerosol instrumentation was operated based on recommendations from the World Calibration Centre for Aerosol Physics (WCCAP) under the World Meteorological Organization's (WMO) Global Atmosphere Watch (GAW) Programme. The sampling was carried out following the guidelines presented in the GAW report 227 (WMO Report, 2016) to minimize particle loss due to diffusion, impaction, and settling. To ensure the accuracy of measurements, the relative humidity during the campaign was maintained below 40%. This was achieved by utilizing a Nafion® Permapure dryer and controlling the temperature within the air-conditioned measurement container to 27°C (Tõnisson et al., 2020). The Manila North Port site (Figure 1a), situated in a key shipping and cargo-handling area, is characterised by emissions from diesel-powered cranes, heavy-duty trucks, and maritime traffic, especially during active loading and unloading times. This semi-open location, positioned near Manila Bay, benefits from higher wind speeds that facilitate pollutant dispersion (Madueño et al., 2019). In contrast, Quezon City's East Avenue roadside (Figure 1b) location experiences dense, regular traffic dominated by light-duty vehicles and public jeepneys, with heavy emissions during peak hours. This urban setting, with close proximity to residential and commercial buildings, likely influences pollutant dispersion patterns and retention due to the built environment (Madueño et al., 2022; Alas et al., 2018; Kecorius et al., 2017). Similar to findings by Grivas et al. (2019), which details BC levels in traffic-heavy avenues, and Kaminska et al. (2023), which examines BC distribution influenced by urban structure, the characterisation of these sites highlights how kerbside features impact pollutant concentrations. These site details enhance our study's relevance to urban BC research and highlight the importance of location-specific factors for effective air quality interventions.

2.2 Instrumentation

2.2.1 Organic and inorganic aerosols

The Aerosol Chemical Speciation Monitor (ACSM, Aerodyne Research Inc., Billerica, MA, USA) was utilised for real-time continuous monitoring of non-refractory submicron particulate matter (NR-PM_1) targeting organic compounds, sulphate (SO_4^{2-}), nitrate (NO_3^-), ammonium (NH_4^+), and chloride (Cl^-) with a detection limit < 0.2 $\mu g/m^3$ at the Port site. It is important to note that while ACSM data from the Port site was used, Quezon City site data was excluded due to its unavailability. This instrument is effective in analysing particles within the vacuum aerodynamic diameter size range of approximately 80 nm to 800 nm, corresponding to a 50% transmission efficiency in the aerodynamic size spectrum from 75–650 nm, with the efficiency dropping to 30–40% at 1 μm (Liu et al., 2007; Atabakhsh et al., 2023). Before the sample aerosol reaches the device, it flows at a flow rate of 1.6 litres per minute through a PM_{10} impactor inlet (custom-made), a 2.5 m long stainless-steel vertical sampling tube (6 mm inner diameter) and a Nafion dryer (MD–110–48S–4, Perma Pure LLC,

Toms River, NJ, USA). ACSM installed an NR–PM_1 internal inlet that eliminated particles larger than 1 μm. In comparison, the dryer maintained a relative humidity below 50% and a flow rate of 1.6 litres per minute minimising particle transport losses in the particle size range of 30 nm to 1 μm. It was expected that particle losses in the system would be less than 2%. The particles of aerosol, inside the ACSM, were focused on a heat-resistant surface at a temperature of 600°C, in which the NR–PM_1 components that were NR–PM_1 were vaporised. The resulting gasses were identified and chemically analysed using 70 eV electron impact quadrupole mass spectrometry (Pauraitė et al., 2015). As the detection takes place via thermal vaporisation at 600°C, the BC is not detectable by ACSM (Tõnisson et al., 2020). The instrument was run with a time resolution of 30 minutes and a mass spectrometer scan rate of 220 (amu/s), from m/z 12 to 149, for normal aerosol loadings (a few $\mu g/m^3$). ACSM standard data analysis software (v 1.5.3.0) and DAQ 1.4.4.4 were used to process the aerosol mass concentration and mass spectra (Tõnisson et al., 2020). Ammonium nitrate (NH_4NO_3) and ammonium sulphate (NH_4)$2SO_4$ were used for periodic calibration of the device (Tõnisson et al., 2020). The following calibration parameters were set during the calibration of the device: RIENO_3 = 1.1, RIENH_4 = 9.14, RIESO_4 = 4.2, RIEOrg = 1.4, and RIEChl= 1.3, and the response factor was equal to 2.26×10^{-11}. The resulting particle counting efficiency (CE) was evaluated based on the method suggested by Middlebrook et al. (2012) and was equal to 0.5.

2.2.2 Equivalent black carbon

The measurements of black carbon aerosol were carried out by an Aethalometer (model AE31, Magee Scientific, Berkeley, CA, USA, Helin et al., 2018; Liu et al., 2018). It measures the optical transmission of carbonaceous aerosol particles through the filter at seven wavelengths λ (370, 450, 520, 590, 660, 880 and 950 nm). It is considered that absorption of light at a wavelength of 880 nm represents BC in the atmosphere as it is the main absorbent of light in this channel (Bodhaine, 1995; Lavanchy et al., 1999), while other known aerosol components have a negligible effect (Weingartner et al., 2003; Zotter et al., 2017). The AE31 converts the light attenuation into the eBC mass concentration by using the MAC value of 16.6 $m^2\ g^{-1}$ at a wavelength of 880 nm (standard parameter according to the manufacturer's specifications). The sampling inlet is located 4 m above the ground and is equipped with a $PM_{2.5}$ cut-size impactor model SCC 1.828 (BGI Co.) operating at 4 litres per minute. It is known that filter-based optical measurements suffer from the filter-loading effect (Park et al., 2010). The eBC mass concentration exhibits a linear correlation with its attenuation. However, as filter loading increases, the sensitivity of the filter's attenuation response reduces, consequently leading to an underestimation of the actual eBC concentrations. The main filter-loading correction methods were described in the article by Collaud et al. (2010). In this study, the eBC data were corrected for the effects of filter loading using an empirical algorithm (Virkkula et al., 2007). The data was compiled into an hourly mean dataset for analysis. Negative values in the hourly mean eBC data were removed following the averaging process. Routine calibration tests of the AE31 determined that the detection limit for eBC mass concentration is below 40 ng/m^3, operating at a measurement resolution of 5 minutes.

2.2.3 Distinction between traffic- and biomass-related eBC

The 'Aethalometer model' developed by Sandradewi et al. (2008) was used to differentiate the eBC mass concentrations originating from biomass burning (eBC_{BB}) and fossil fuels (eBC_{FF}). This model utilizes the absorption Ångström exponent (AAE) at specific wavelengths (470 and 880 nm) to allocate the BC concentration to its respective source.

$$b_{abs,BC_{BB}}(880\,nm) = \frac{b_{abs}(470\,nm) - \left(\frac{470}{880}\right)^{AAE_{BB}}}{\left(\frac{470}{880}\right)^{AAE_{TR}} - \left(\frac{470}{880}\right)^{AAE_{BB}}} \quad (1)$$

$$b_{abs,BC_{TR}}(880\,nm) = \frac{(b_{abs}(470\,nm) - \left(\frac{470}{880}\right)^{AAE_{TR}}}{\left(\frac{470}{880}\right)^{AAE_{BB}} - \left(\frac{470}{880}\right)^{AAE_{TR}}} \quad (2)$$

The selection of AAE values for traffic (AAE_{TR}) and biomass burning (AAE_{BB}) follows comprehensive studies that examined similar urban settings with dominant traffic and biomass burning sources such as Zotter et al. (2017), Qin et al. (2018), Cappa et al. (2012, 2016), Pauraite et al. (2020), Minderytė et al. (2022) and Byčenkienė et al. (2023). These values are 0.9 for AAE_{TR} and 1.68 for AAE_{BB}, as identified by Zotter et al. (2017) through extensive measurements and eBC source apportionment analysis across various European locations, ensuring applicability to urban environments similar to Manila. This study's AAE for black carbon (AAE_{BC}) of 1.43 was chosen based on its alignment with Zotter et al. (2017), Dumka et al. (2018) and Pauraite et al. (2020), which analyzed environments impacted by significant fossil fuel and biomass burning sources, similar to the conditions observed in Manila.

Further support for the AAE values used in this study is drawn from Minderytė et al. (2022) and Byčenkienė et al. (2023), who also reported similar AAE values under comparable urban pollution conditions. These findings emphasise the relevance and robustness of the AE31 model in distinguishing between biomass and traffic-related black carbon. Additionally, although direct sensitivity analysis has not been performed due to constraints in this study, referencing works such as Kaskaoutis et al. (2021) confirmed the robustness of the Aethalometer model across different urban environments. In our previous work by Byčenkienė et al. (2023), we have conducted sensitivity

analysis which supports the reliability of the AAE values adopted. The AAE values adopted are supported by multiple sources and are consistent with those used in related literature, ensuring a reliable source apportionment in the Manila context.

Brown carbon (BrC) was investigated based on the AAE wavelength dependence method (WDA) proposed by Wang et al. (2016). This method is based on an assumption that light absorption at 880 nm represents only BC while absorption at 370 nm could be related to both eBC and BrC light absorption. WDA method can be expressed as follows:

$$\mathrm{AAE}^{\mathrm{BC}}_{370/880} = \mathrm{AAE}_{660/880} + \mathrm{WDA} \tag{3}$$

$$\mathrm{b_{abs,BC}}(370\,\mathrm{nm}) = \mathrm{b_{abs}}(880\,\mathrm{nm}) - \frac{880}{370}^{\mathrm{AAE_{BC}}} \tag{4}$$

$$\mathrm{b_{abs,BrC}}(370\,\mathrm{nm}) = \mathrm{b_{abs}}(370\,\mathrm{nm}) - \mathrm{b_{abs,BC}}(370\,\mathrm{nm}) \tag{5}$$

The technique applied here operates on the assumption that light absorption at 370 nm could be related to both BC and BrC absorption, while light absorption at 880 nm solely reflects BC absorption (Pauraite et al., 2020). The analysis also takes into account minor dust absorption at 370 nm as mentioned by Zhao et al. (2019) and Kaskaoutis et al. (2021).

2.2.4 Aerosol particle number size distribution

For particle number size distribution within a size range from 0.5 to 10.0 μm and number concentration assessment, an aerodynamic particle sizer (APS – model 3221, TSI Inc., USA; TSI, Inc. 2004) was used. It is worth noting that while the APS accurately determines the aerodynamic diameter for most aerosol particles (Bartley et al., 2000), its counting efficiency (CE) exhibits variability and is influenced by particle size, as demonstrated by Preifer et al. (2016). For $PM_{2.5}$ and PM_{10} calculation, we estimated the aerosol mass-weighted aerodynamic concentration by utilizing the APS data, which provided number-weighted particle size distributions (Peters et al., 2006; Pauraite et al., 2021):

$$\mathrm{dM_{D_{ae}}} = \mathrm{dN_{D_{ae}}} \frac{\pi}{6} \mathrm{D^3_{ae}} \left(\frac{\rho_0 \, \mathrm{C_{ae}} X}{\mathrm{C_{ve}}} \right)^{3/2} \frac{1}{(\rho_\mathrm{p})^{1/2}} \tag{6}$$

where, $\mathrm{D_{ae}}$ is the aerodynamic diameter, $\mathrm{dN_{D_{ae}}}$ differential number concentration for a given aerodynamic diameter, ρ_p is the density of the particle, $\mathrm{D_{ve}}$ is the volumetric equivalent diameter which can be calculated from the definition of terminal velocity (Hinds, 1998), ρ_0 is unit density (1 g cm^{-3}), X is the dynamic shape factor, $\mathrm{C_{ae}}$ – Cunningham correction factor associated with aerodynamic diameter, and $\mathrm{C_{ve}}$ – Cunningham correction factor associated with volume equivalent diameter (Zhou et al., 2017). The aerodynamic diameter is converted into the volumetric equivalent diameter for this purpose (Hinds, 1982). According to (Salcedo, 2006), the aerosol particle density, ρp, was estimated to be 1.80 g cm^{-3}, and the shape factor X was also assumed to be 1.9 (Park et al., 2004).

2.2.5 Meteorological conditions

The prevailing wind patterns at the Port and QCG sites are shown in Figure 2. At the Port site (Figure 2a), the predominantly winds originated from the north (N), northeast (NE), and north-north-east (N-NE) directions. Conversely, at the QCG site (Figure 2b), winds primarily originated from the west (W), southwest (SW), and south-south-west (S-SW) directions. Average T and RH at the Port site were 27.54 ± 1.75°C and 68.99 ± 8.49% (Figure 2c and Table 1) and at the QCG site – 26.58 ± 2.95°C and 66.45 ± 11.57% (Figure 2d and Table 1). The number after "±" shows the standard deviation.

2.2.6 Quality assurance

To ensure the data quality of the aerosol measurements, we strictly adhered to the protocols described in our previous studies, such as those outlined by Alas et al. (2018). For example, the instruments and aerosol containers were checked daily throughout the campaign. Every two weeks, the aerosol flow of the individual instruments and the main inlet system was measured to identify possible leaks. Before and after the move to another location, the flow rates of the instruments in the aerosol container were also thoroughly checked to ensure consistent operation under different conditions. Extending these detailed measures, the data quality of aerosol measurements was further ensured by adhering to World Meteorological Organization guidelines for aerosol measurements (e.g. aerosol drying below 40% RH using membrane dryers; using PM_{10} inlet to protect aerosol sampling lines from contamination; keeping sampling lines conductive, vertical and short to minimise aerosol losses). Furthermore, total flow and instrument-specific flow zero checks, high voltage calibration and aerosol particle sizing accuracy (using polystyrene latex standard of 200, 1000 and 2000 nm; for mobility measurement-based devices and aerodynamic particle sizer), and instrument flows were tested on a weekly bases. The Aerosol Chemical Speciation Monitor (ACSM) was calibrated by using the ACSM calibration protocol (Williams et al., 2021).

3. Results and discussion

3.1 Overview of organic and inorganic aerosols

The time series of hourly average non-refractory particulate matter (NR-PM_1) species at the Port site are shown in Figure 3a. The total PM_1 mass concentration of the non-refractory species measured by the ACSM ranged from a few μg/m^3, with the maximum hourly average reach-

Table 1. The average temperature (T; °C), relative humidity (RH; %), wind direction (WD; °), wind speed (WS; m/s) and pressure (hPa) during the measurement campaign at the Port site and QCG site.

Site		T (°C)	RH (%)	WS (m/s)	WD (°)	Pressure (hPa)
Port Site	Mean	27.54	68.99	1.44	134.05	1013.29
	Median	27.4	70	1.3	90	1013.2
	SD	1.75	8.49	1.03	112.05	2.38
	Max	34.3	92	6.3	337.5	1019.6
	Min	23.1	42	0	0	1007.1
QCG Site	Mean	26.58	66.45	0.31	211.18	1010.80
	Median	26.2	67	0.4	247.5	1010.8
	SD	2.95	11.57	0.36	112.87	1.95
	Max	34.7	93	2.2	337.5	1016.1
	Min	19.7	35	0	0	1004.9

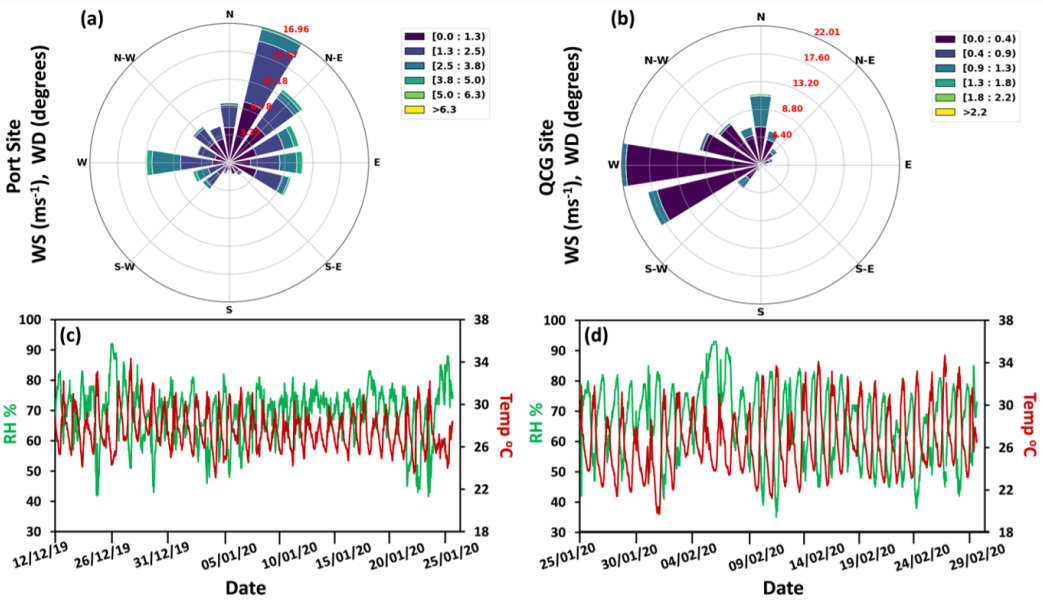

Figure 2. Wind diagrams showing the wind direction, wind speed and frequency at Port site (a) and QCG site (b). Time series data of ambient temperature (°C) and relative humidity (%) at the Port site (c) and the QCG site (d) throughout the measurement campaign.

ing up to 99.50 $\mu g/m^3$. Throughout the campaign, organic aerosol (OA) emerged as the predominant component of NR-PM_1, constituting a mean hourly average of 80% (23.68 ± 16.40 $\mu g/m^3$). While sulphate constituted the second-largest fraction of 10% (3.14 ± 2.60 $\mu g/m^3$) of the total NR-PM_1 mass (Figure 3a). Notably, nitrates and ammonium exhibited an equivalent contribution of 4% each (1.90 ± 1.32 $\mu g/m^3$ and 1.23 ± 1.02 $\mu g/m^3$) to the total NR-PM_1 mass (Figure 3a). In contrast, chloride represented a minor fraction, ~ 2% (0.47 ± 0.78 $\mu g/m^3$) (Figure 3a). Comparable studies conducted at different locations provide additional insight into the composition of NR-PM_1. The study conducted by Stavroulas et al. (2021) in the port city of Piraeus, Greece similarly highlights a higher concentration of OA (67%) than inorganics such as SO_4^{2-} (19%), NH_4^+ (7%), NO^3 (6%), and Cl^- (1%) in urban atmospheric compositions. In a study conducted by Gani et al. (2019) in Delhi, India, OA similarly dominated and accounted for 50% of NR-PM_1 mass. Ammonium, chloride, and nitrate individually constituted approximately 10%, while sulphate contributed roughly 5% to the NR-PM_1 mass. Another study conducted in Delhi, India by Patel et al. (2021) showed a higher fraction of OA (78%) and a lower fraction of sulphate (20%). Similarly, Warden et al. (2022) in their research in Kathmandu, Nepal observed that average NR-PM_1 was composed by mass of OA (35%), SO_4^{2-} (21%), NH_4^+ (7%), NO_3 (3%), and Cl^- (2%). Nitrate aerosols are primarily formed through the oxidation of nitrogen oxides (NOx), which are significant traffic-related pollutants (Draxler et al., 1998). NOx gases, predominantly emitted from vehicle exhausts, react with other atmospheric components under sunlight to form

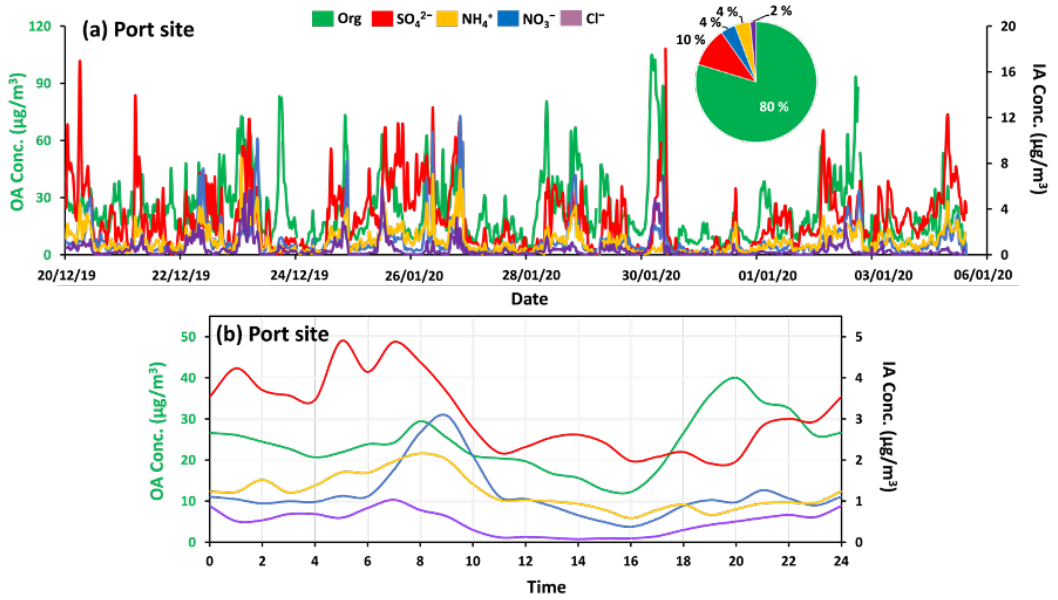

Figure 3. The hourly average temporal variation of species (organics, sulphate, nitrate, ammonium, and chloride) at the Port site. The pie chart shows the fractional abundances of individual ACSM species averaged (a) and diurnal patterns of the organics and inorganics species (SO_4^{2-}, NH_4^+, NO_3^-, and Cl^-) (b) at the Port site.

secondary inorganic aerosols such as nitrates. The concentration of these pollutants is notably higher in urban areas with dense traffic,

3.2 Diurnal analysis of organic and inorganic aerosol particles

At the Port site, the diurnal trend analysis was performed for organic aerosols (OA) and other species including SO_4^{2-}, NH_4^+, NO_3^-, and Cl–. This analysis indicated that OA showed higher mass concentration peaks (29.43 $\mu g/m^3$ and 40.02 $\mu g/m^3$) during morning hours (about 8 am) and late-night hours (about 8 pm). Whereas, a lower mass concentration (12.22 $\mu g/m^3$) was observed between 3 pm–4 pm (Figure 2b). Sulphates showed a higher mass concentration (4.89 $\mu g/m^3$) during morning hours (5 am–7 am) and a lower mass concentration (1.91 $\mu g/m^3$) during evening hours (7 pm–8 pm) (Figure 2b). The formation of SO_4^{2-}–derived aerosol was likely occurring by the oxidation of SO_2 which is the gaseous precursor. This is followed by particle formation through condensation. The study conducted by Cadondon et al. (2024) indicated that SO_4^{2-} ions at Manila North Port mostly originated from ship emissions and marine port vessels. Nitrates, ammonium, and chloride showed higher mass concentrations (3.08 $\mu g/m^3$, 2.16 $\mu g/m^3$, and 1.03 $\mu g/m^3$ respectively) during morning hours (7 am–10 am), whereas lower mass concentrations (0.37 $\mu g/m^3$, 0.58 $\mu g/m^3$, and 0.07 $\mu g/m^3$ respectively) were observed between 2 pm–4 pm (Figure 2b). Similar findings have been consistently demonstrated across various Asian sites. For instance, Gani et al. (2019) conducted research in India, revealing diurnal variations in aerosol composition. They observed higher concentrations around 7 am–8 am and again around 9 pm–10 pm , with lower concentrations typically occurring around 3 pm–4 pm. In addition to this, Werden et al. (2022) studies in Nepal revealed that higher concentrations of organic aerosols (OA) occurred in the morning hours and late evening around 8 pm, coinciding with typical peak traffic hours and mealtimes. Inorganic aerosols, such as NO_3^-, SO_4^{2-}, and Cl^-, also exhibited higher concentrations in the morning hours and lower concentrations during midday. The increased concentration of SO_4 in the morning was attributed to traffic and industrial emissions, while lower concentrations were associated with an increase in wind speed. Similarly, studies conducted in Bangladesh (Salam et al., 2008) and Pakistan (Alam et al., 2011) highlighted diurnal patterns in aerosol constituents, underscoring the significance of regional variations in aerosol dynamics.

3.3 Mass concentration of equivalent black carbon (eBC)

The measurement campaign revealed that the eBC mass concentration was higher at the QCG site than at the Port site. The mean hourly average eBC mass concentration at the Port site was 10.27 ± 5.99 $\mu g/m^3$, while the mean hourly average mass concentration at the QCG site was 35.97 ± 16.20 $\mu g/m^3$, as shown in Figure 4a and b, respectively. The maximum hourly average eBC mass concentration reached up to 35.82 $\mu g/m^3$ at the Port site and 104.54 $\mu g/m^3$ at the QCG site. In the Philippines, particularly in urban centres like Metro Manila, different studies utilising AE31data have unveiled the alarming presence

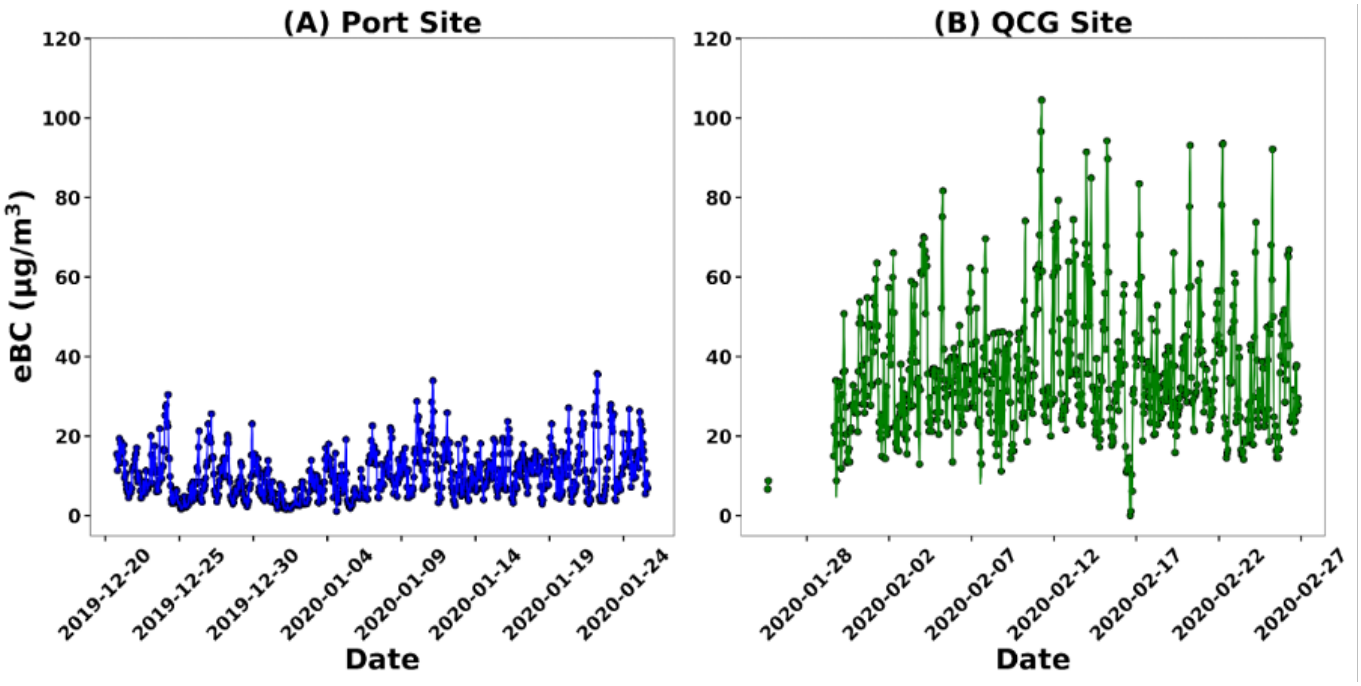

Figure 4. Time series of hourly average eBC mass concentration at Port site (a) and QCG site (b) (AE 31), during the measurement campaign.

of elevated eBC concentrations. For example, studies conducted by Alas et al. (2018) and Madueño et al. (2022) revealed that higher eBC mass concentrations were attributed to emissions from vehicles and industrial activities in the region. According to Madueño et al. (2022), a five-month study in Manila, Philippines revealed that eBC mass concentrations are 2 to 17 times higher than those in urban and traffic areas of India, China, Europe, and the USA. The annual average eBC concentration, however, remains undetermined. Our study corroborates these findings, as our results also show higher eBC concentrations compared to other sites. Building on this discussion, recent findings by Cadondon et al. (2024) at Manila Port reported that atmospheric particle pollution is predominantly from local anthropogenic sources, such as ship emissions and industrial activities. Moreover, their air mass backward trajectories analysis indicated that, although air masses originated from the Pacific in the Southeast region of the study area, high factor loadings were of local anthropogenic origins.

Beyond the Philippines, other Asian countries have also struggled with elevated eBC levels, often associated with rapid urbanisation and industrial expansion. Notably, research conducted by Kumar et al. (2020), Dumka et al. (2019, 2019) and Bisht et al. (2019) in India, Bilal et al. (2022) in Pakistan, Quang et al. (2021) in Vietnam, Chen et al. (2019) in China, and Shakya et al. (2017) in Nepal highlighting the influence of traffic and industrial sources on eBC concentrations. When we compare our results to findings from previous studies, it is clear that urban and industrial emissions consistently influence higher eBC levels in different regions. Factors like local regulations and the intensity of industrial activities also play significant roles. For instance, the eBC levels at our QCG site are quite higher than those found in densely populated urban areas of India and Nepal, mainly due to traffic and industrial emissions. On the other hand, the lower eBC levels at the Port site indicate stricter local regulations or lower industrial activity. Differences in measurement approaches used in various studies also contribute to discrepancies in reported levels. Therefore, it is crucial to implement customised strategies that take into account specific urban characteristics and regulatory environments to effectively reduce eBC pollution and improve public health. Table 2 provides a comparative analysis of the daily average eBC mass concentrations observed at these sites against the backdrop of global research, emphasising the pressing need for effective emission reduction measures.

3.4 Source apportionment of equivalent black carbon (eBC)

The source apportionment of eBC originating from traffic and biomass burning was rigorously examined by utilizing the Absorption Ångström Exponent for transport (AAE_{TR}) and Absorption Ångström Exponent for biomass burning (AAE_{BB}) values, as mentioned in Section 2.2.3. Figure 5a and b show the hourly average time series and the contributions of eBC_{TR} and eBC_{BB} to the overall eBC mass concentration at the Port site and QCG site, respectively. The percentage contribution reveals that at the Port site eBC_{TR} and eBC_{BB} accounted for 86% and 14%, respec-

Table 2. Comparative analysis of mean hourly and daily averages, maximum daily and hourly concentration values, and diurnal trends of various airborne pollutants at the Port site and QCG site, highlighting differences in pollutant levels between the different sites.

	Instrument	Mean Hourly Average ($\mu g/m^3$)	Max Hourly Conc Value ($\mu g/m^3$)	Mean Daily Average ($\mu g/m^3$)	Max Daily Conc Value ($\mu g/m^3$)	Max Diurnal Trend ($\mu g/m^3$)	Min Diurnal Trend ($\mu g/m^3$)	Reference
OA (Port)	ACSM	23.68 ± 16.40	99.50	23.36 ± 8.94	40.47	29.43	12.22	(this study)
SO42– (Port)	ACSM	3.09 ± 2.60	18.0	3.14 ± 1.55	6.84	4.89	1.91	(this study)
NO3– (Port)	ACSM	1.18 ± 1.32	11.20	1.18 ± 0.52	2.01	3.08	0.37	(this study)
NH4+ (Port)	ACSM	1.19 ± 1.02	6.96	1.20 ± 0.56	2.26	2.16	0.58	(this study)
Cl– (Port)	ACSM	0.47 ± 0.78	6.90	0.47 ± 0.28	1.15	1.03	0.07	(this study)
eBC (Port)	(AE31)	10.27 ± 5.99	35.82	10.32 ± 3.01	15.25	15.57 ± 3.46	5.05	(this study)
eBC (QCG)	(AE31)	35.97 ± 16.20	104.54	34.08 ± 7.29	44.25	63.45 ± 10.61	23.43	(this study)
eBC (Port)	(AE33)	16 ± 3	70.21					Cadondon et al. (2024)
eBC Manila (PHL)	(AE33)			25.7				Alas et al. (2018)
eBC (Quezon, PHL)	(AE33)			36.7				Madueño et al. (2022)
eBC (Delhi, India)	(AE31)			13.57				Kumar et al. (2020)
eBC (Delhi, India)	(AE33)			7.2				Dumka et al. (2019)
eBC (Delhi, India)	(AE33)			14.91				Dumka et al. (2019)
eBC (Delhi, India)	(AE33)			7.89				Bisht et al. (2019)
eBC (Lahore, PAK)	(AE33)			21.7				Bilal et al. (2022)
eBC, (Hanoi, Vietnam)	(AE33)			32.5				Quang et al. (2021)
eBC (Guangzhou, China)	(AE31)			20.5				Chen et al. (2019)
eBC (Kathmandu, Nepal)	(AE33)			15				Shakya et al. (2017)
eBC_{BB} (Port)	(AE31)	1.28 ± 0.72	5.73	1.28 ± 0.61	5.73	1.86 ± 0.26	0.77	(this study)
eBC_{TR} (Port)	(AE31)	7.75 ± 5.34	35.39	$7.88 \pm 4.31\ 3$	5.39	12.24 ± 3.05	3.65	(this study)
eBC (Port)	(AE31)	8.36 ± 5.92	43.50	8.47 ± 4.80	43.50			(this study)
BrC (Port)	(AE31)	2.06 ± 2.10	26.10	2.06 ± 1.68	26.10			(this study)
eBC_{BB} (QCG)	(AE31)	6.06 ± 2.24	17.52	5.90 ± 2.13	17.52	8.49 ± 1.0	4.79	(this study)
eBC_{TR} (QCG)	(AE31)	24.95 ± 14.85	102.48	24.08 ± 12.67	102.48	47.69 ± 9.34	13.97	(this study)
eBC (QCG)	(AE31)	28.16 ± 14.59	102.90	27.31 ± 12.92	102.90			(this study)
BrC (QCG)	(AE31)	7.77 ± 3.44	24.58	7.57 ± 3.26	24.58			(this study)
$PM_{2.5}$ (Port)	APS	32.24 ± 14.25	92.98	92.98				(this study)
PM_{10} (Port)	APS	47.45 ± 19.20	117.95	117.95				(this study)
$PM_{2.5}$ (QCG)	APS	85.38 ± 36.52	236.37	236.37				(this study)
PM_{10} (QCG)	APS	129.46 ± 51.20	273.34	273.34				(this study)

tively, of the total eBC mass concentration (Figure 5a). Similarly, at the QCG site eBC_{TR} and eBC_{BB} contributed 80% and 20%, respectively, to the overall eBC mass concentration (Figure 5b). Notably, the dominant contributor to eBC was eBC_{TR} at both sites throughout the measurement campaign. The small variation in eBC source apportionment between the two sites can be attributed to distinct emissions profiles linked to each location. At the Port site, where eBC_{TR} constituted the majority, the predominant source of eBC was likely related to vehicle emissions from heavy-duty trucks, trollers and diesel-powered cranes. Furthermore, the Port's infrastructure contributes significantly as one of the main sources of eBC. At the QCG site, where eBC_{TR} also played a more substantial role, the primary source of eBC was likely linked to pollution stemming from on-road transport. The urban landscape of Quezon City typically features a dense network of roads, and traffic-related emissions, especially from vehicles such as diesel-powered Jeepneys (PUJs) and light-duty vehicles (LDVs) (Kecorius et al., 2017; Madueño et al., 2019; Alas et al., 2018).

eBC and BrC have different spectral dependencies, with brown carbon being expected to absorb strongly in the UV range. Figure 5c–d depicts the hourly average time series and contribution of the light absorption coefficients of eBC and BrC at the Port site and QCG site, respectively. The light absorption coefficient of BrC at 370 nm ($b_{abs,BrC}$) varied spatially from 0.02 to 0.80 M m^{-1}. The $b_{abs,BC}$ showed a slightly higher contribution of 80% and 78% to light absorption at a lower wavelength (370 nm) at the Port site and QCG site, respectively (Figure 5c–d). Whereas, the contribution of BrC was only 20% and 22% at the Port site and QCG site, respectively (Figure 5c–d). According to studies conducted at the Quezon City site by Tun et al. (2019), Salvador et al. (2022), and Pabroa et al. (2022), significant sources of biomass-burning-derived eBC include domes-

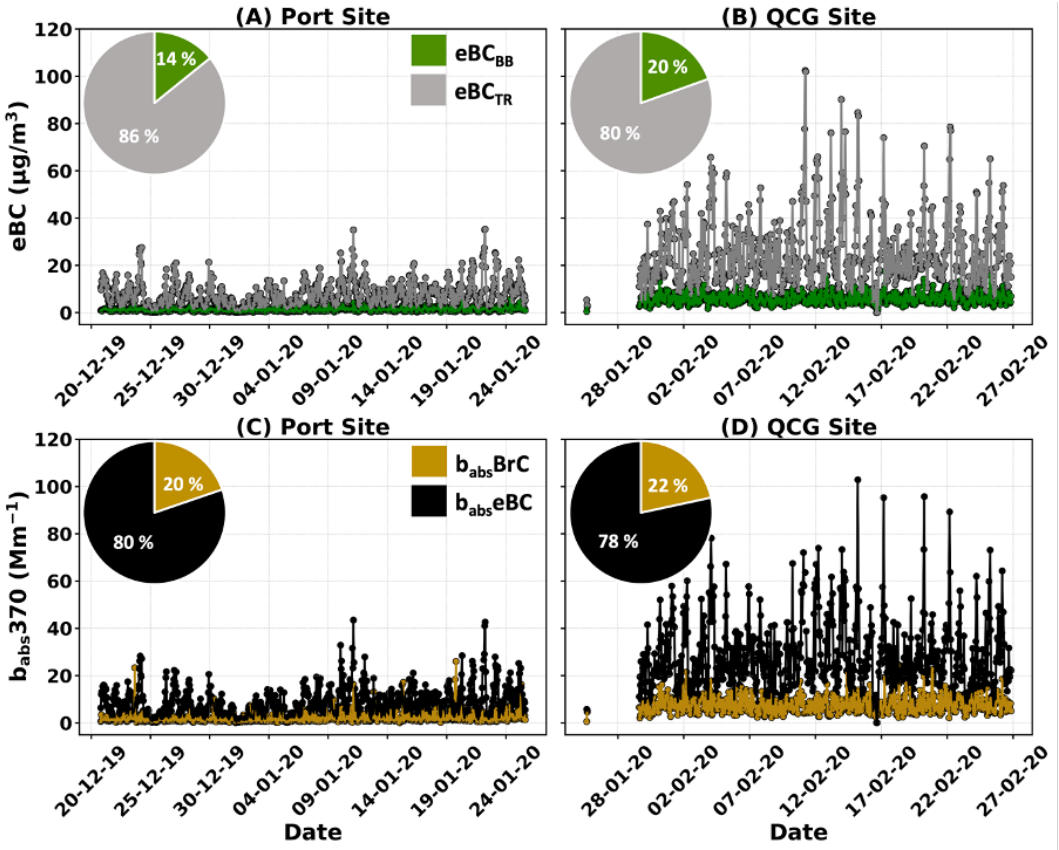

Figure 5. Time series and contributions of the hourly average eBC_{TR} and eBC_{BB} to the total eBC at Port site (A) and QCG site (B); b_{abs} BrC and b_{abs} BC to the total $b_{abs}(Mm^{-1})$ at Port site (C) and QCG site (D). Time series and contributions of the hourly average eBC_{TR} and eBC_{BB} to the total eBC at Port site (A) and QCG site (B); b_{abs} BrC and b_{abs} BC to the total b_{abs} (Mm^{-1}) at Port site (C) and QCG site (D).

tic and commercial cooking, particularly involving charcoal. Additionally, studies carried out by Liu et al. (2018) and Qin et al. (2018) have shown that biomass burning during cooking activities was the main source of BrC in Quezon City. Whereas, at the Port site, distant agricultural activities and waste incineration are major sources of biomass burning-derived eBC, with the long-range transport of these pollutants also playing a significant role (Ulevičius et al., 2010). Notably, although vital, shipping and maritime operations at Port sites are not directly related to biomass burning emissions, they primarily contribute to the combustion of fuels and the release of particulate matter (Geng et al., 2024). On the other hand, the primary source of BrC at the Port site was also linked to biomass burning, specifically from waste incineration, agricultural burning, and shipping and maritime operations.

The BC and BrC contributions presented in this study, along with those from various urban locations worldwide, are compared in Figure S2. In this study, BrC contributions of 20% and 22% were observed at the Port and QCG sites, respectively. These values are comparable to those reported in other urban locations such as Manaus, Brazil; Singapore; Lyon, France; Kathmandu, Nepal; and Guangzhou, China, which reported BrC contributions of 15%, 15%, 20%, 25%, and 25%, respectively (De Sá et al., 2019; Kasthuriarachchi et al., 2020; Zhang et al., 2020a; Kim et al., 2021; Qin et al., 2018). Similar to our study sites, fossil fuel and traffic-related emissions were identified as the main contributors in these locations, with lower contributions from biomass-burning sources. In contrast, lower BrC contributions were observed in other urban areas. For instance, Panyu, Xianlin, and Xianghe in China reported BrC contributions of 2%, 5%, and 10%, respectively, while Athens, Greece, and Gwangju, Korea, both recorded contributions of 10% (Li et al., 2019; Liakaou et al., 2019; Wang et al., 2018b; Yang et al., 2009; Park et al., 2019). The variation in BrC contribution across different urban locations (Figure S2) likely reflects differences in primary emission sources, types of combustion, and prevailing meteorological conditions in these regions. On the other hand, higher BrC contributions were observed in several European and Asian urban areas. For example, Bordeaux, Nantes, Rouen, Poitiers, Marseille, Reims, and Grenoble in France each reported BrC contributions of 30%, while Chiang Mai, Thailand, and Beijing, China, reported values of 45% and 46%, respectively (Zhang et al., 2020a; Pani et al., 2021; Xie et al.,

2019) (Figure S2). These elevated BrC levels are primarily attributed to residential wood burning and biomass burning, indicating that these areas are significantly influenced by these combustion sources.

3.5 Diurnal analysis of eBC, eBC_{TR} and eBC_{BB}

The hourly average diurnal trend analysis for eBC, eBC_{TR} and eBC_{BB} was performed at both the Port site and the QCG site. The analysis indicated that eBC, eBC_{TR} and eBC_{BB} exhibited similar diurnal patterns at both measurement sites, as shown in Figure 6A and B, respectively. At the QCG site, the highest eBC mass concentration was noted at 63.45 ± 10.61 $\mu g/m^3$ during the morning hours (6 am –8 am), with the lowest concentration of 23.43 ± 10.61 $\mu g/m^3$ occurring midday (11 am–1 pm). At the Port site, the peak eBC mass concentration was lower, reaching up to 15.57 ± 3.46 $\mu g/m^3$ in the morning and declining to 5.05 ± 3.46 $\mu g/m^3$ at midday. Additionally, at the QCG site, the highest eBC_{TR} mass concentration (47.69 ± 9.34 $\mu g/m^3$) was observed during the morning hours (6 am –8 am), and the lowest concentration (13.97 ± 9.34 $\mu g/m^3$) was noted around midday (11 am–1 pm). Furthermore, another significant peak of 30.63 ± 9.34 $\mu g/m^3$ for eBC_{TR} was recorded late at night (10 pm–12 am). At the QCG site in the morning rush hours, eBC_{TR} higher mass concentration may be ascribed to enhanced traffic emissions from cars and jeepneys, whereas late at night higher concentration may mostly be associated with emissions from diesel trucks. The heavy diesel trucks, which are major emission sources of eBC_{TR}, were allowed to enter the city from 10 pm to 7 am and banned during morning rush hours (Alas et al., 2018) therefore less emission was observed than morning rush hours. Furthermore, different factors such as increased mixing layer and higher wind speed (Figure S1) decreased the eBC_{TR} concentration during daytime at the QCG site. Whereas, during late night hours lower wind speed (Figure S1) and lower mixing layer enhanced eBC_{TR} concentration. The eBC_{BB} exhibited a diurnal trend that was quite similar to BCTR. The highest eBC_{BB} mass concentration at the QCG site (8.49 ± 1.0 $\mu g/m^3$) was observed during the morning hours (6 am–8 am) and the lowest concentration (4.79 ± 1.0 $\mu g/m^3$) during midday (11 am–1 pm). In many regions, especially in urban and suburban areas, resident engage in morning activities such as cooking breakfast, which often involves the burning of biomass fuels like wood or agricultural waste (Salvador et al., 2022). This localized biomass burning can lead to elevated eBC_{BB} levels during the early hours. In addition, atmospheric mixing can also influence the dispersion and concentration of pollutants. During midday, increased turbulence and mixing may disperse pollutants more effectively, leading to a decline in observed concentrations.

At the Port site, the higher concentration of eBC_{TR} (12.24 ± 3.05 $\mu g/m^3$) occurred during the morning hours (6 am–8 am), while the lowest concentration (3.65 ± 3.05 $\mu g/m^3$) was recorded during midday (11 am–1 pm). It can be assumed that at the Manila Port site, a decreased concentration of eBC_{TR} during the central diurnal hours is due to the cycle of the planetary boundary layer height (Cesari et al., 2018). At the Manila Port, in the morning hours, elevated concentrations of black carbon (eBC_{TR}) can be attributed to several key factors. Heavy-duty diesel vehicles, such as trucks and buses, play a substantial role as they transport goods to and from the Port, with exhaust emissions surging during the morning rush hours (Bagtasa et al., 2020; Miller et al., 2023). Maritime traffic is a further contributor as many ships are employing diesel engines that emit black carbon, especially during manoeuvres near the Port (Alas et al., 2018). Additionally, cargo handling equipment, often diesel-powered, is active in the morning, and traffic congestion, along with road dust resuspension, exacerbates inefficient combustion, collectively leading to higher concentrations of black carbon. In the afternoon at the Manila Port site, traffic-related black carbon concentrations typically decrease due to reduced morning rush hour traffic, improved traffic flow and increased mixing layer.

The diurnal pattern of eBC_{BB} was quite similar to eBC_{TR}, with the peak eBC_{BB} concentration (1.86 ± 0.26 $\mu g/m^3$) occurring during the morning hours (6 am–8 am) and the lowest concentration (0.77 ± 0.26 $\mu g/m^3$) recorded during midday (11 am–1 pm). The higher concentration of eBC_{BB} at the Port site during the morning hours can be attributed to several factors such as lower turbulent mixing and wind patterns (e.g., the measurement site is downwind of the pollutant source during morning hours). During the midday, enhance vertical and horizontal mixing disperse pollutants, diminishing surface concentrations) (Deng et al., 2020). In a study conducted in Manila, Philippines, by Madueño et al. (2019), the diurnal trend of eBC showed a similar pattern to the results obtained in this study. The highest eBC mass concentration was observed during the morning hours (6 am–8 am), and the lowest was observed during the afternoon (2 pm–4 pm). Similarly, a study conducted in Beijing, China, by Nie et al. (2022) reported a significant increase in BC mass concentration during the morning rush hours, indicating the impact of traffic emissions on air quality

3.6 $PM_{2.5}$ and PM_{10} mass concentration

The $PM_{2.5}$ and PM_{10} shown in Figure 7(A and B) illustrate the hourly average mass concentrations at both the Port and QCG sites. Notably, at the Port site, mean hourly average mass concentrations of $PM_{2.5}$ was (32.24 ± 14.25 $\mu g/m^3$) and PM_{10} (47.45 ± 19.20 $\mu g/m^3$) were observed. It is important to highlight that the mean hourly average mass concentration of $PM_{2.5}$, measured at 32.24 $\mu g/m^3$ at the Port site, exceeded both the WHO guideline of 15 $\mu g/m^3$ and the limit value set by the Philippines Clean Air Act of 2016 (50 $\mu g/m^3$). However, the mean hourly average

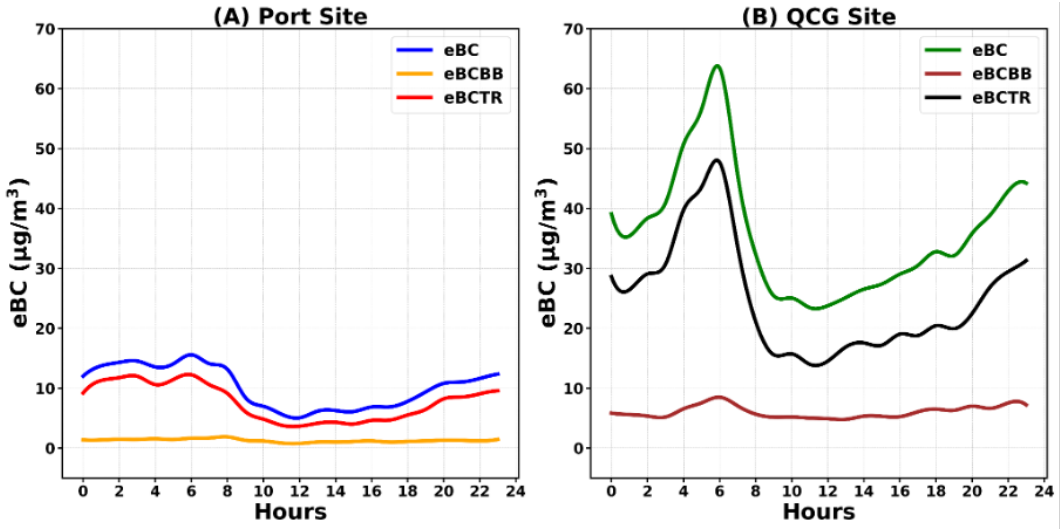

Figure 6. The diurnal pattern of eBC, eBC_{TR} and eBC_{BB} at Manila Port site (a) and QCG site (b), during the measurement campaign.

mass concentration of PM_{10}, which was 47.45 $\mu g/m^3$, remained within the permissible limits set by the WHO guideline (50 $\mu g/m^3$) and outlined in the Philippines Clean Air Act of 1999 (150 $\mu g/m^3$). The maximum hourly average mass concentrations of $PM_{2.5}$ and PM_{10} were observed at 92.98 $\mu g/m^3$ and 117.95 $\mu g/m^3$, respectively, at the port site. Recent findings by Cadondon et al. (2024) reported similar results, indicating that mean air pollutant concentrations at Manila Port exceed the 24-hour Philippine guidelines due to ship operations.

At the QCG site, the mean hourly average mass concentrations of $PM_{2.5}$ and PM_{10} were even higher, reaching values of (85.38 ± 36.52 $\mu g/m^3$) and (129.46 ± 51.20 $\mu g/m^3$), respectively. It is worth noting that, similar to the Port site, the mean hourly average concentration of $PM_{2.5}$ at the QCG site exceeded both the WHO guideline of 15 $\mu g/m^3$ and the limit set by the Philippines Clean Air Act of 2016 (50 $\mu g/m^3$). Likewise, the PM_{10} concentration, while exceeding the WHO guideline of 50 $\mu g/m^3$, remained within the 150 $\mu g/m^3$ limit prescribed by the Philippines Clean Air Act of 1999. The maximum hourly average mass concentrations of $PM_{2.5}$ and PM_{10} were observed reaching up to 236.37 $\mu g/m^3$ and 273.34 $\mu g/m^3$, respectively, at the QCG site.

To further understand the particulate matter composition and pollution sources, the analysis of the eBC to PM ratios at both sites was conducted. At the Port site, the eBC to $PM_{2.5}$ ratio and eBC to PM_{10} ratio were determined to be 0.35 (35%) and 0.24 (24%), respectively (Table S2). In comparison, the QCG site exhibited a higher proportion of eBC, with ratios of 0.42 (42%) for eBC to $PM_{2.5}$ and 0.27 (27%) for eBC to PM_{10} (Table S2). This suggests that the QCG site may be more influenced by combustion-related particulate matter, possibly from vehicular traffic, industrial activities, or biomass burning prevalent in urban settings. Additionally, the source apportionment analysis corroborates these findings, indicating a significant contribution from traffic-related black carbon. These findings collectively indicate a highly concerning level of particulate matter pollution at both the Port and QCG sites.

These observations are supported by recent studies, which highlight the role of local vehicular and shipping emissions in high eBC concentrations, particularly intense at the Port site and along congested urban corridors (Cadondon et al., 2024; Madueño et al., 2022; Alas et al., 2018). Furthermore, the presence of soot particles, mainly within the $PM_{2.5}$ size range, significantly contributes to the $PM_{2.5}$ mass, supporting the high eBC percentages reported in this study (Kecerious et al., 2017). According to Cadondon et al. (2024), at Manila North Port, the mean share of eBC in $PM_{2.5}$ is 18%, indicating that the eBC/$PM_{2.5}$ ratios recorded in Manila North Harbour are higher compared to other urban areas globally, highlighting that fine to quasi-fine particles in Manila North harbour were largely emitted by the anthropogenic activities and associated BC. The geographic and climatic conditions of Metro Manila, such as its coastal location and high annual precipitation, typically lead to lower PM_{10} concentrations but do not similarly affect finer particles like $PM_{2.5}$, which regularly exceed WHO limits (Oanh et al., 2006; Zhu et al., 2012). This results in a disproportionately high level of eBC within the finer particulate fraction ARE, reflecting similar findings from Cruz et al. (2023) and previous traffic-related studies in Metro Manila (Madueño et al., 2019; Kecorius et al., 2017, 2019).

In addition, we examined the influence of meteorological parameters on PM concentrations. The analysis revealed that daily average temperature (27°C), relative humidity (68%), and atmospheric pressure (1013 hPa) were quite similar at both sites (Table 1). However, wind speed

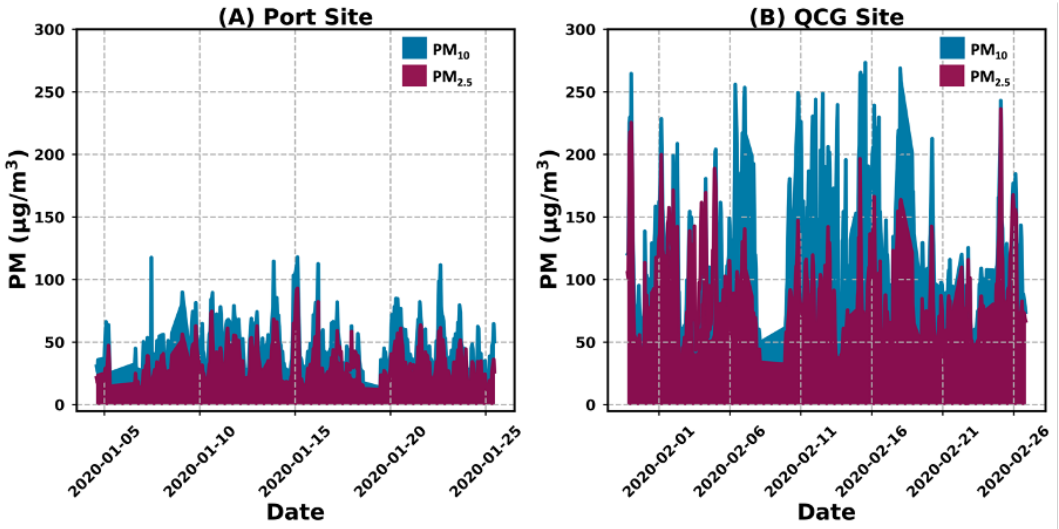

Figure 7. Time series of hourly average mass concentration of $PM_{2.5}$ (dark red) and PM_{10} (cerulean), during measurement campaign at Port site (a) and QCG site (b).

was higher at the Port site compared to the QCG site, which may contribute to the lower PM concentrations observed there. Despite this, the correlation analysis (Table S1) following the methodology of Schober et al. (2018), indicated negligible correlations between these meteorological factors and $PM_{2.5}$ and PM_{10} levels at both sites, suggesting other factors such as local industrial activities and traffic emissions play more significant roles in determining PM levels. Manila North Port's air quality is comparatively better than Quezon City due to its closeness to Manila Bay as higher wind speed helps to disperse contaminants. Furthermore, the natural diffusing effects of sea breezes together with the higher relative humidity lower the pollution levels at marine and coastal locations (Plauškaitė et al., 2017). In addition to that Manila's North Harbour does have some industrial activity such as transporting cargo, but industrial emissions, such as those from manufacturing and construction, are less concentrated here than in Quezon City, which has a more varied industrial environment. To address the high levels of $PM_{2.5}$ and PM_{10} at the Port and QCG sites, we recommend stricter emission standards for vehicles, regular inspections and maintenance for heavy-duty vehicles (Kecorius et al., 2017). In addition, banning public service vehicles such as jeepneys (Alas et al., 2018), expanding air quality monitoring in Manila and improving green infrastructure are crucial (Madueño et al., 2019; Cruz et al., 2023). These measures, combined with legislative support and community engagement, are essential to improve urban air quality and public health.

4. Limitations of the study and future work

Our study provides detailed insights into the sources and concentrations of carbonaceous aerosols in Manila North Port and the urban environment of Quezon City. By focusing on eBC, it highlights the urgent need for effective air quality management in urban environments. However, it is important to note that the data collection period in this study does not cover all seasonal variations that could affect air quality. Seasonal variations are known to significantly affect particulate matter concentrations. While the monitoring locations were carefully selected, they only represent two specific urban areas and may not reflect broader geographic variations within or outside Metro Manila. In addition to that, ACSM data was only analyzed for the Port site and not for the QCG site, which may limit the comprehensiveness of our findings. Future studies should aim to produce comprehensive data with a wide geographic range to strengthen the foundation for managing air quality and developing policies. Furthermore, Mass Absorption Coefficient (MAC), shape, and density values were considered as the limitation of this study because they were not previously measured but assumed from current literature. Although these assumptions might impact the precision of our findings, they do not drastically alter the main conclusion: eBC concentrations are extremely high in Metro Manila. Additionally, our study was constrained by the use of the Aerodynamic Particle Sizer (APS), which measures particles only within a limited size range up to 0.6 μm. This restricts our ability to fully characterise finer particulate matter components, particularly those below this size threshold that contribute significantly to $PM_{2.5}$ concentrations. This constraint may lead to potential underestimations of total particulate matter, especially finer fractions that are critical for health impact assessments in urban environments. For future work, we propose to integrate the use of the Aerodynamic Particle Sizer (APS) and the Scanning Mobility Particle Sizer (SMPS) to ensure a comprehensive coverage of the size range of particulate matter. While the APS effectively measures larger particles

in the 0.5 μm to 20 μm range, the SMPS excels at capturing the size distribution of much finer particles, typically from 10 nm to 1 μm. This two-instrument approach will improve our characterization of particulate matter in the air and increase our understanding of health impacts in urban areas.

5. Conclusion

This study investigates air pollution and its sources in an urban environment, specifically at Quezon City's East Avenue roadside and Manila's North Port, Philippines, from December 20, 2019, to February 26, 2020. At the Port site organics were the primary component (80%) of non-refractory submicron aerosols (NR-PM_1), followed by sulphate (10%), nitrate (4%), ammonium (4%), and chloride (2%). Furthermore, organic aerosols showed higher mass concentrations during morning hours (6 am–8 am) and lower during midday (3 pm–4 pm), while inorganic aerosols peaked from 5 am to 10 am and lower concentrations were observed between 2 pm to 4 pm. The measurements indicated that the eBC mass concentration was notably higher at the QCG site compared to the Port site. Specifically, the daily average eBC concentration at the QCG site is 3 times higher than at the Port site. Compared to other Asian cities such as Kathmandu and Hanoi but slightly lower than in Delhi and Guangzhou, indicating significant health risks for commuters. Further analysis revealed that eBC_{TR} contributed significantly more to both the Port and QCG sites, accounting for 86% and 80% of eBC, respectively, compared to eBC_{BB} (14% and 20%, respectively). The biomass-burning-related eBC contribution was further supported by an analysis of BrC. The babs eBC presented a higher contribution at both Port and QCG sites (80% and 78% respectively) and babs BrC presented a lower contribution of 20% and 22%, respectively. This emphasizes the dominant role of the transport sector as the primary source of black carbon in urban areas. Diurnal analysis of eBC_{TR} and eBC_{BB} revealed similar patterns at both the Port and QCG sites. The highest mass concentrations (47.69 ± 9.34 $\mu g/m^3$) of eBC_{TR} were consistently observed during the morning rush hours (6 am–8 am), mostly attributed to the emissions from diesel-powered Jeepneys (PUJs) and light-duty vehicles (LDVs), while late-night high concentration (30.63 ± 9.34 $\mu g/m^3$) peaks were associated with emissions from heavy diesel trucks at QCG site, as it is allowed only at nighttime to regulate air pollution in the city. During the day, only light-duty vehicles and public transport traffic is allowed. Whereas, at the Port site, the higher concentration (12.24 ± 3.05 $\mu g/m^3$) peak of eBC_{TR} in morning hours (6 am–8 am) was attributed to the emissions from heavy-duty trucks, trollers, diesel-powered cranes and ships. The proximity of Manila North Port to Manila Bay plays a pivotal role in its relatively cleaner air quality, benefiting from the higher wind speed causing greater air mixing and causatively the higher dispersion of pollutants. Consequently, coastal areas typically experience lower pollution levels due to the natural diffusion effect of greater air mixing in the boundary layer and higher relative humidity leading to more efficient removal of pollutants from the atmosphere. Furthermore, higher $PM_{2.5}$ and PM_{10} mass concentrations were recorded at the QCG site compared to the Port site. Alarmingly, the study found that not only did $PM_{2.5}$ and PM_{10} exceed WHO guidelines and the Philippines Clean Air Act limit values, but also eBC was noticeably higher than those values at both sites. This study provides extended insights into air pollution characteristics in the megacity of Metro Manila, which can be incorporated into urban air quality models and health studies. It underscores the necessity of developing better indicators to evaluate air quality where pollution is driven by BC emissions. It is recommended to implement monitoring of the main air pollutants in Metro Manila on a regular basis.

Credit statement

Touqeer Gill: Investigation, Methodology, Formal analysis, and Writing – Original Draft, Kamilė Kandrotaitė, Vadimas Dudoitis: Investigation and Validation, Simonas Kecorius, Laurent Poulain, Leizel Madueño: Resources, Investigation, Formal analysis, Writing – Review and Editing, Alfred Wiedensohler, Edgar A. Vallar, Maria Cecilia D. Galvez: Resources Supervision, Steigvilė Byčenkienė, Kristina Plauškaitė: Writing – Review, Editing and Supervision.

Acknowledgements

This research was funded by the German Federal Ministry of Education and Research in the framework of TAME-BC (project number 01LE1903A). Simonas Kecorius acknowledges funding from the Research Council of Lithuania (LMTLT), agreement No. S-MIP-22-57. All authors have read and agreed to the published version of the manuscript.

Conflict of interest

None declared.

Supplementary materials

Please follow this link to see the supplementary material associated with this article.

References

Alam, K., Blaschke, T., Madl, P., Mukhtar, A., Hussain, M., Trautmann, T., Rahman, S., 2011. *Aerosol size distribution and mass concentration measurements in various cities of Pakistan*. J. Environ. Monit. 13, 1944–1952. https://doi.org/10.1039/c1em10086f

Alas, H.D., Müller, T., Birmili, W., Kecorius, S., Cambaliza, M.O., Simpas, J.B.B., Cayetano, M., Weinhold, K., Vallar,

E., Galvez, M.C., Wiedensohler, A., 2018. *Spatial characterization of black carbon mass concentration in the atmosphere of a southeast Asian megacity: An air quality case study for metro Manila, Philippines*. Aerosol Air Qual. Res. 18, 2301–2317. https://doi.org/10.4209/aaqr.2017.08.0281

Atabakhsh, S., Poulain, L., Chen, G., Canonaco, F., Prévôt, A.S.H., Pöhlker, M., Wiedensohler, A., Herrmann, H., 2023. *A 1-year aerosol chemical speciation monitor (ACSM) source analysis of organic aerosol particle contributions from anthropogenic sources after long-range transport at the TROPOS research station Melpitz*. Atmos. Chem. Phys. 23, 6963–6988. https://doi.org/10.5194/acp-23-6963-2023

Bartley, D.L., Martinez, A.B., Baron, P.A., Secker, D.R., Hirst, E., 2000. *Droplet distortion in accelerating flow*. J. Aerosol Sci. 31, 1447–1460. https://doi.org/10.1016/S0021-8502(00)00042-2

Bagtasa, G., Yuan, C.S., 2020. *Influence of local meteorology on the chemical characteristics of fine particulates in Metropolitan Manila in the Philippines*. Atmos. Pollut. Res. 11, 1359–1369. https://doi.org/10.1016/j.apr.2020.05.013

Bilal, M., Ali, M.A., Nichol, J.E., Bleiweiss, M.P., de Leeuw, G., Mhawish, A., Shi, Y., Mazhar, U., Mehmood, T., Kim, J., Qiu, Z., Qin, W., Nazeer, M. 2022. *AEROsol generic classification using a novel Satellite remote sensing Approach (AEROSA)*. Front. Environ. Sci. 10:981522. https://doi.org/10.3389/fenvs.2022.981522

Bisht, D.S., Dumka, U.C., Kaskaoutis, D.G., Pipal, A.S., Srivastava, A.K., Soni, V.K., Attri, S.D., Sateesh, M., Tiwari, S. 2015. *Carbonaceous aerosols and pollutants over Delhi urban environment: Temporal evolution, source apportionment and radiative forcing*. Sci. Total Environ. 521–522, 431–445. https://doi.org/10.1016/j.scitotenv.2015.03.083

Bodhaine, B.A., 1995. *Aerosol absorption measurements at Barrow, Mauna Loa and the south pole*. J. Geophys. Res. 100, 8967–8975. https://doi.org/10.1029/95JD00513

Braun, R.A., Aghdam, M.A., Bañaga, P.A., Betito, G., Cambaliza, M.O., Cruz, M.T., Lorenzo, G.R., Macdonald, A.B., Simpas, J.B., 2020. *Long-range aerosol transport and impacts on size-resolved aerosol composition in Metro Manila, Philippines*. Atmos. Chem. Phys. 20, 2387–2405, https://doi.org/10.5194/acp-20-2387-2020

Byčenkienė, S., Gill, T., Khan, A., Kalinauskaitė, A., Ulevicius, V., Plauškaitė, K., 2023. *Estimation of Carbonaceous Aerosol Sources under Extremely Cold Weather Conditions in an Urban Environment*. Atmosphere 14. https://doi.org/10.3390/atmos14020310

Carslaw, D.C., 2005. *Evidence of an increasing NO2/NOX emissions ratio from road traffic emissions*. Atmos. Environ. 39, 4793–4802. https://doi.org/10.1016/j.atmosenv.2005.06.023

Cadondon, J., Caido, N.G., Galvez, M.C., Rempillo, O., Esmeria Jr., J., Vallar, E., 2024. *Black carbon and PM0.49 characterization in Manila North Harbour Port, Metro Manila, Philippines*. Environ. Adv. 16, 100526. https://doi.org/10.1016/j.envadv.2024.100526

Cappa, C.D., Onasch, T.B., Massoli, P., Worsnop, D.R., Bates, T.S., Cross, E.S., Davidovits, P., Hakala, J., Hayden, K.L., Jobson, B.T., Kolesar, K.R., Lack, D.A., Lerner, B.M., Li, S.-M., Mellon, D., Nuaaman, I., Olfert, J.S., Petäjä, T., Quinn, P.K., Song, C., Subramanian, R., Williams, E.J., Zaveri, R.A., 2012. *Response to Comment on "Radiative Absorption Enhancements Due to the Mixing State of Atmospheric Black Carbon"*. Science 339(6118), 393-c. https://doi.org/10.1126/science.1230260

Cappa, C.D., Kolesar, K.R., Zhang, X., Atkinson, D.B., Pekour, M.S., Zaveri, R.A., Zelenyuk, A., Zhang, Q., 2016. *Understanding the optical properties of ambient sub- and supermicron particulate matter: results from the CARES 2010 field study in northern California*. Atmos. Chem. Phys. 16, 6511–6535. https://doi.org/10.5194/acp-16-6511-2016

Cesari, D., Merico, E., Dinoi, A., Marinoni, A., Bonasoni, P., Contini, D., 2018. *Seasonal variability of carbonaceous aerosols in an urban background area in Southern Italy*. Atmos. Res. 200, 97–108. https://doi.org/10.1016/j.atmosres.2017.10.004

Chen, X., Zhang, Z., Engling, G., Zhang, R., Tao, J., Lin, M., Sang, X., Chan, C., Li, S., Li, Y., 2014. *Characterization of fine particulate black carbon in Guangzhou, a megacity of south China*. Atmos. Pollut. Res. 5, 361–370. https://doi.org/10.5094/APR.2014.042

Cohen, A.J., Brauer, M., Burnett, R., Anderson, H.R., Frostad, J., Estep, K., Balakrishnan, K., Brunekreef, B., Dandona, L., Dandona, R., Feigin, V., Freedman, G., Hubbell, B., Jobling, A., Kan, H., Knibbs, L., Liu, Y., Martin, R., Morawska, L., Pope, C.A., Shin, H., Straif, K., Shaddick, G., Thomas, M., van Dingenen, R., van Donkelaar, A., Vos, T., Murray, C.J.L., Forouzanfar, M.H., 2017. *Estimates and 25-year trends of the global burden of disease attributable to ambient air pollution: an analysis of data from the Global Burden of Diseases Study 2015*. Lancet 389, 1907–1918. https://doi.org/10.1016/S0140-6736(17)30505-6

Collaud Coen, M., Weingartner, E., Apituley, A., Ceburnis, D., Fierz-Schmidhauser, R., Flentje, H., Henzing, J.S., Jennings, S.G., Moerman, M., Petzold, A., Schmid, O., Baltensperger, U., 2010. *Minimizing light absorption measurement artifacts of the Aethalometer: evaluation of five correction algorithms*. Atmos. Meas. Tech. 3, 457–474. https://doi.org/10.5194/amt-3-457-2010

Cruz, M.T., Simpas, J.B., Sorooshian, A., Betito, G., Cambaliza, M.O.L., Collado, J.T., Eloranta, E.W., Holz, R., Topacio, X.G.V., Del Socorro, J., Bagtasa, G., 2023. *Impacts*

of regional wind circulations on aerosol pollution and planetary boundary layer structure in Metro Manila, Philippines. Atmos. Environ. 293, 119455. https://doi.org/10.1016/j.atmosenv.2022.119455

Deng, J., Guo, H., Zhang, H., Zhu, J., Wang, X., Fu, P., 2020. *Source apportionment of black carbon aerosols from light absorption observation and source-oriented modeling: An implication in a coastal city in China*. Atmos. Chem. Phys. 20, 14419–14435. https://doi.org/10.5194/acp-20-14419-2020

De Sa, S.S., Rizzo, L.V., Palm, B.B., Campuzano-Jost, P., Day, D.A., Yee, L.D., Wernis, R., Isaacman-VanWertz, G., Brito, J., Carbone, S., Liu, Y.J., Sedlacek, A., Springston, S., Goldstein, A.H., Barbosa, H.M.J., Alexander, M.L., Artaxo, P., Jimenez, J.L., Martin, S.T., 2019. *Contributions of biomass-burning, urban, and biogenic emissions to the concentrations and light-absorbing properties of particulate matter in central Amazonia during the dry season*. Atmos. Chem. Phys., 19, 7973–8001. https://doi.org/10.5194/acp-19-7973-2019

Donaldson, K., Gilmour, M.I., Macnee, W., 2000. *Commentary Asthma and PM 10*. Respir. Res. 1, 12–15.

Draxler, R.R., Hess, G.D., 1998. *An overview of the HYSPLIT_4 modelling system for trajectories, dispersion and deposition*. Aust. Meteorol. Mag. 47, 295–308.

Dumka, U.C., Kaskaoutis, D.G., Tiwari, S., Safai, P.D., Attri, S.D., Soni, V.K., Singh, N., Mihalopoulos, N., 2018. *Assessment of biomass burning and fossil fuel contribution to black carbon concentrations in Delhi during winter*. Atmos.Environ. 194, 93–109. https://doi.org/10.1016/j.atmosenv.2018.09.033

Dumka, U.C., Kaskaoutis, D.G., Devara, P.C.S., Kumar, R., Kumar, S., Tiwari, S., Gerasopoulos, E., Mihalopoulos, N., 2019. *Year-long variability of the fossil fuel and wood burning black carbon components at a rural site in southern Delhi outskirts*. Atmos. Res. 216, 11–25. https://doi.org/10.1016/j.atmosres.2018.09.016

Dumka, U.C., Tiwari, S., Kaskaoutis, D.G., Soni, V.K., Safai, P.D., Attri, S.D., 2019. *Aerosol and pollutant characteristics in Delhi during a winter research campaign*. Environ. Sci. Pollut. Res. 26, 3771–3794. https://doi.org/10.1007/s11356-018-3885-y

Fan, M., Zhang, W., Zhang, Y., Li, J., Fang, H., Al, F.A.N.E.T., 2023. *Formation Mechanisms and Source Apportionments of Nitrate Aerosols in a Megacity of Eastern China Based On Multiple Isotope Observations*. J. Geophys. Res.-Atmos. 1–14. https://doi.org/10.1029/2022JD038129

Gani, S., Bhandari, S., Seraj, S., Wang, D.S., Patel, K., Soni, P., Arub, Z., Habib, G., Hildebrandt Ruiz, L., Apte, J.S., 2019. *Submicron aerosol composition in the world's most polluted megacity: The Delhi Aerosol Supersite study*. Atmos. Chem. Phys. 19, 6843–6859. https://doi.org/10.5194/acp-19-6843-2019

Geng, X., Li, J., Zhong, G., Zhao, S., Tian, C., Zhang, Y.-L., Zhang, G., 2024. *Ship Emissions as the Largest Contributor to Coastal Atmospheric Black Carbon at a Receptor Island in Southern China*. Environ. Sci. Technol. Lett. 11, 723–729. https://doi.org/10.1021/acs.estlett.4c00362

Grivas, G., Stavroulas, I., Liakakou, E., Kaskaoutis, D.G., Bougiatioti, A., Paraskevopoulou, D., Gerasopoulos, E., Mihalopoulos, N., 2019. *Measuring the spatial variability of black carbon in Athens during wintertime*. Air Quality, Atmos. Health 12, 1459–1470. https://doi.org/10.1007/s11869-019-00756-y

Helin, A., Niemi, J. V., Virkkula, A., Pirjola, L., Teinilä, K., Backman, J., Aurela, M., Saarikoski, S., Rönkkö, T., Asmi, E., Timonen, H., 2018. *Characteristics and source apportionment of black carbon in the Helsinki metropolitan area, Finland*. Atmos. Environ. 190, 87–98. https://doi.org/10.1016/j.atmosenv.2018.07.022

Hinds, W.C. 1982. *Aerosol Technology: Properties, Behavior and Measurement of Airborne Particles*. John Wiley & Sons, Hoboken.

Hinds, W.C., 1998. *Aerosol Technology: Properties, Behavior and Measurement of Airborne Particles*. John Wiley & Sons, Hoboken.

Kaminska, J.A., Turek, T., Van Poppel, M., Peters, J., Hofman, J., Kazak, J.K., 2023. *Whether cycling around the city is in fact healthy in the light of air quality – Results of black carbon*. J. Environ. Manage. 337, 117694. https://doi.org/10.1016/j.jenvman.2023.117694

Kasthuriarachchi, N.Y., Rivellini, L.H., Adam, M.G., Lee, A.K.Y., 2020. *Light absorbing properties of primary and secondary brown carbon in a tropical urban environment*. Environ. Sci. Technol., 54, 10808–10819. https://doi.org/10.1021/acs.est.0c02414

Kaskaoutis, D.G., Grivas, G., Stavroulas, I., Bougiatioti, A., Liakakou, E., Dumka, U.C., Gerasopoulos, E., Mihalopoulos, N., 2021. *Apportionment of black and brown carbon spectral absorption sources in the urban environment of Athens, Greece, during winter*. Sci. Total Environ. 801, 149739. https://doi.org/10.1016/j.scitotenv.2021.149739

Kaskaoutis, D.G., Grivas, G., Stavroulas, I., Liakakou, E., Dumka, U.C., Gerasopoulos, E., Mihalopoulos, N., 2021. *Effect of aerosol types from various sources at an urban location on spectral curvature of scattering and absorption coefficients*. Atmospheric Research, 264, 105865. https://doi.org/10.1016/j.atmosres.2021.105865

Kecorius, S., Madueño, L., Löndahl, J., Vallar, E., Cecilia, M., Idolor, L.F., Gonzaga-Cayetano, M., Müller, T., Birmili, W., Wiedensohler, A., 2019. *Science of the Total Environment Respiratory tract deposition of inhaled roadside ultra fine refractory particles in a polluted megacity of South-East Asia*. Sci. Total Environ. 663, 265–274. https://doi.org/10.1016/j.scitotenv.2019.01.338

Kecorius, S., Madueño, L., Vallar, E., Alas, H., Betito, G., Birmili, W., Cambaliza, M.O., Catipay, G., Gonzaga-Cayetano, M., Galvez, M.C., Lorenzo, G., Müller, T., Simpas, J.B., Tamayo, E.G., Wiedensohler, A., 2017. *Aerosol particle mixing state, refractory particle number size distributions and emission factors in a polluted urban environment: Case study of Metro Manila, Philippines*. Atmos. Environ. 170, 169–183. https://doi.org/10.1016/j.atmosenv.2017.09.037

Kim, S.W., Cho, C., Rupakheti, M., 2021. *Estimating contributions of black and brown carbon to solar absorption from aethalometer and AERONET measurements in the highly polluted Kathmandu Valley, Nepal*. Atmos. Res., 247, 105164. https://doi.org/10.1016/j.atmosres.2020.105164

Kumar, R.R., Soni, V.K., Jain, M.K., 2020. *Evaluation of spatial and temporal heterogeneity of black carbon aerosol mass concentration over India using three-year measurements from IMD BC observation network*. Sci. Total Environ. 723, 138060. https://doi.org/10.1016/j.scitotenv.2020.138060

Lavanchy, V.M.H., Gäggeler, H.W., Schotterer, U., Schwikowski, M., Baltensperger, U., 1999. *Historical record of carbonaceous particle concentrations from a European high-alpine glacier (Colle Gnifetti, Switzerland)*. J. Geophys. Res. Atmos. 104, 21227–21236. https://doi.org/10.1029/1999JD900408

Lelieveld, J., Evans, J.S., Fnais, M., Giannadaki, D., Pozzer, A., 2015. *The contribution of outdoor air pollution sources to premature mortality on a global scale*. Nature 525, 367–371. https://doi.org/10.1038/nature15371

Liu, P.S.K., Deng, R., Smith, K.A., Williams, L.R., Jayne, J.T., Canagaratna, M.R., Moore, K., Onasch, T.B., Worsnop, D.R., Deshler, T., 2007. *Transmission efficiency of an aerodynamic focusing lens system: Comparison of model calculations and laboratory measurements for the aerodyne aerosol mass spectrometer*. Aerosol Sci. Technol. 41, 721–733. https://doi.org/10.1080/02786820701422278

Liu, C., Chung, C.E., Yin, Y., Schnaiter, M., 2018. *The absorption Ångström exponent of black carbon: From numerical aspects*. Atmos. Chem. Phys. 18, 6259–6273. https://doi.org/10.5194/acp-18-6259-2018

Li, Z., Tan, H., Zheng, J., Liu, L., Qin, Y., Wang, N., Li, F., Li, Y., Cai, M., Ma, Y., Chan, C.K., 2019. *Light absorption properties and potential sources of particulate brown carbon in the Pearl River Delta region of China*. Atmos. Chem. Phys., 19, 11669–11685. https://doi.org/10.5194/acp-19-11669-2019

Liakakou, E., Kaskaoutis, D.G., Grivas, G., Stavroulas, I., Tsagkaraki, M., Paraskevopoulou, D., Bougiatioti, A., Dumka, U.C., Gerasopoulos, E., Mihalopoulos, N. 2020. *Long-term brown carbon spectral characteristics in a Mediterranean city (Athens)*. Sci. Total Environ. 708, 135019. https://doi.org/10.1016/j.scitotenv.2019.135019

Madueño, L., Kecorius, S., Birmili, W., Müller, T., Simpas, J., Vallar, E., Galvez, M.C., Cayetano, M., Wiedensohler, A., 2019. *Aerosol particle and black carbon emission factors of vehicular fleet in Manila, Philippines*. Atmosphere (Basel). 10. https://doi.org/10.3390/atmos10100603

Madueño, L., Kecorius, S., Löndahl, J., Schnelle-Kreis, J., Wiedensohler, A., Pöhlker, M., 2022. *A novel in-situ method to determine the respiratory tract deposition of carbonaceous particles reveals dangers of public commuting in highly polluted megacity*. Part. Fibre Toxicol. 19. https://doi.org/10.1186/s12989-022-00501-x

Merico, E., Dinoi, A., Contini, D., 2019. *Development of an integrated modelling-measurement system for near-real-time estimates of harbour activity impact to atmospheric pollution in coastal cities*. Transp. Res. Pt. D 73, 108–119. https://doi.org/10.1016/j.trd.2019.06.009

Middlebrook, A.M., Bahreini, R., Jimenez, J.L., Canagaratna, M.R., 2012. *Evaluation of composition-dependent collection efficiencies for the Aerodyne aerosol mass spectrometer using field data*. Aerosol Sci. Technol. 46, 258–271. https://doi.org/10.1080/02786826.2011.620041

Miller, R.M., Rauber, R.M., Di Girolamo, L., Rilloraza, M., Fu, D., Mcfarquhar, G.M., Nesbitt, S.W., Ziemba, L.D., Woods, S., Thornhill, K.L., 2023. *Influence of natural and anthropogenic aerosols on cloud base droplet size distributions in clouds over the South China Sea and West Pacific*. Atmos. Chem. Phys. 23, 8959–8977. https://doi.org/10.5194/acp-23-8959-2023

Minderytė, A., Pauraite, J., Dudoitis, V., Plauškaitė, K., Kilikevičius, A., Matijošius, J., Rimkus, A., Kilikevičienė, K., Vainorius, D., Byčenkienė, S., 2022. *Carbonaceous aerosol source apportionment and assessment of transport-related pollution*. Atmos. Environ. 279. https://doi.org/10.1016/j.atmosenv.2022.119043

Myllyvirta, L., Suarez, I., 2020. *Air quality and health impacts of coal-fired power in the Philippines*.

Nie, D., Qiu, Z., Wang, X., Liu, Z., 2022. *Characterizing the source apportionment of black carbon and ultrafine particles near urban roads in Xi'an, China*. Environ. Res. 215, 114209. https://doi.org/10.1016/j.envres.2022.114209

Oanh, N.T., Upadhyay, N., Zhuang, Y.H., Hao, Z.P., Murthy, D.V.S., Lestari, P., Villarin, J.T., Chengchua, K., Co, H.X., Dung, N.T., Lindgren, E.S., 2006. *Particulate air pollution in six Asian cities: Spatial and temporal distributions, and associated sources*. Atmos. Environ. 40, 3367–3380. https://doi.org/10.1016/j.atmosenv.2006.01.050

Pabroa, P.C.B., Racho, J.M.D., Jagonoy, A.M., Valdez, J.D.G., Bautista VII, A.T., Yee, J.R., Pineda, R., Manlapaz, J., Atanacio, A.J., Coronel, I.C. V., Salvador, C.M.G., Cohen, D.D., 2022. *Characterization, source apportionment and associated health risk assessment of respirable air particulates in Metro Manila, Philippines*. Atmos. Pollut. Res. 13, 101379. https://doi.org/10.1016/j.apr.2022.101379

Park, S., Yu, G.H., 2019. *Absorption properties and size distribution of aerosol particles during the fall season at an urban site of Gwangju, Korea*. Environ. Eng. Res. 24, 159–172. https://doi.org/10.4491/eer.2018.166

Pani, S.K., Lin, N.-H., Griffith, S.M., Chantara, S., Lee, C.-T., Thepnuan, D., Tsai, Y.I., 2021. *Brown carbon light absorption over an urban environment in northern peninsular Southeast Asia*. Environ. Pollut. 276, 116735. https://doi.org/10.1016/j.envpol.2021.116735

Patel, K., Bhandari, S., Gani, S., Campmier, M.J., Kumar, P., Habib, G., Apte, J., Hildebrandt Ruiz, L., 2021. *Sources and Dynamics of Submicron Aerosol during the Autumn Onset of the Air Pollution Season in Delhi, India*. ACS Earth Sp. Chem. 5, 118–128. https://doi.org/10.1021/acsearthspacechem.0c00340

Park, K., Kittelson, D.B., McMurry, P.H., 2004. *Structural properties of diesel exhaust particles measured by Transmission Electron Microscopy (TEM): Relationships to particle mass and mobility*. Aerosol Sci. Technol. 38, 881–889. https://doi.org/10.1080/027868290505189

Park, S.S., Hansen, A.D.A., Cho, S.Y., 2010. *Measurement of real-time black carbon for investigating spot loading effects of Aethalometer data*. Atmos. Environ. 44, 1449–1455. https://doi.org/10.1016/j.atmosenv.2010.01.025

Pauraite, J., Mainelis, G., Kecorius, S., Minderytė, A., Dudoitis, V., Garbarienė, I., Plauškaitė, K., Ovadnevaite, J., Byčenkienė, S., 2021. *Office indoor PM and BC level in Lithuania: The role of a long-range smoke transport event*. Atmosphere (Basel) 12. https://doi.org/10.3390/atmos12081047

Peters, T.M., Ott, D., O'Shaughnessy, P.T., 2006. *Comparison of the Grimm 1.108 and 1.109 portable aerosol spectrometer to the TSI 3321 aerodynamic particle sizer for dry particles*. Ann. Occup. Hyg. 50, 843–850. https://doi.org/10.1093/annhyg/mel067

Pfeifer, S., Müller, T., Weinhold, K., Zikova, N., Dos Santos, S.M., Marinoni, A., Bischof, O.F., Kykal, C., Ries, L., Meinhardt, F., Aalto, P., Mihalopoulos, N., Wiedensohler, A., 2016. *Intercomparison of 15 aerodynamic particle size spectrometers (APS 3321): Uncertainties in particle sizing and number size distribution*. Atmos. Meas. Tech. 9, 1545–1551. https://doi.org/10.5194/amt-9-1545-2016

Philippine Land Transportation Office Annual Report, 2023. *Philippine Land Transportation Office Annual Rep.*, Philippine Gov. https://lto.gov.ph/wp-content/uploads/2023/11/Annual_Reports-2023.pdf, (Last access: 17 February 2024).

Philippine Population Density, 2015. *Philippine Population Density*, (based on the 2015 Census of Population), Philippine Gov. https://psa.gov.ph/system/files/phcd/202212/Cities%2520and%2520Municipalities%2520Population%2520Projections_2015CBPP_Phils.pdf, (Last access: 17 February 2024).

Philippines, Environmental Management Bureau, 2018. *National Air Quality Status Report 2016–2018*. Dep. Environ. Nat. Res., Environ.l Manage. Bureau, Philippines. https://air.emb.gov.ph/wp-content/uploads/2021/01/National-Air-Quality-Status-Report-2008-2015_With-message-from-D.pdf

Plauškaitė, K., Špirkauskaitė, N., Byčenkienė, S., Kecorius, S., Jasinevičienė, D., Petelski, T., Zielinski, T., Andriejauskienė, J., Barisevičiūtė, R., Garbaras, A., Makuch, P., Dudoitis, V., Ulevicius, V., 2017. *Characterization of aerosol particles over the southern and South-Eastern Baltic Sea*. Mar. Chem. 190, 13–27. https://doi.org/10.1016/j.marchem.2017.01.003

Qin, Y.M., Bo Tan, H., Li, Y.J., Jie Li, Z., Schurman, M.I., Liu, L., Wu, C., Chan, C.K., 2018. *Chemical characteristics of brown carbon in atmospheric particles at a suburban site near Guangzhou, China*. Atmos. Chem. Phys. 18, 16409–16418. https://doi.org/10.5194/acp-18-16409-2018

Quang, T.N., Hue, N.T., Dat, M. Van, Tran, L.K., Phi, T.H., Morawska, L., Thai, P.K., 2021. *Motorcyclists have much higher exposure to black carbon compared to other commuters in traffic of Hanoi, Vietnam*. Atmos. Environ. 245, 118029. https://doi.org/10.1016/j.atmosenv.2020.118029

Republic of the Philippines, 1999. *Philippine Clean Air Act of 1999: An Act Providing for a Comprehensive Air Pollution Control Policy and for Other Purposes*. 11th Congr. Philipp. Metro Manila. June 23, 1999, 1–29.

Salvador, C.M.G., Yee, J.R. dR., Coronel, I.C. V., Bautista VII, A.T., Sugcang, R.J., Lavapie, M.A.M., Capangpangan, R.Y., Pabroa, P.C.B., 2022. *Variability and Source Characterization of Regional PM of Two Urban Areas Dominated by Biomass Burning and Anthropogenic Emission*. Aerosol Air Qual. Res. 22, 220026. https://doi.org/10.4209/aaqr.220026

Salam, A., Hossain, T., Siddique, M.N.A., Shafiqul Alam, A.M., 2008. *Characteristics of atmospheric trace gases, particulate matter, and heavy metal pollution in Dhaka, Bangladesh*. Air Qual. Atmos. Heal. 1, 101–109. https://doi.org/10.1007/s11869-008-0017-8

Sandradewi, J., Prévôt, A.S.H., Weingartner, E., Schmidhauser, R., Gysel, M., Baltensperger, U., 2008. *A study of wood burning and traffic aerosols in an Alpine valley using a multi-wavelength Aethalometer*. Atmos. Environ. 42, 101–112. https://doi.org/10.1016/j.atmosenv.2007.09.034

Salcedo, D., Onasch, T.B., Dzepina, K., Canagaratna, M.R., Zhang, Q., Huffmann, J.A., DeCarlo, P.F., Jayne, J.T., Mortimer, P., Worsnop, D.R., Kolb, C.E., Johnson, K.S., Zuberi, B., Marr, L.C., Volkamer, R., Molina, L.T., Molina, M.J., Cardenas, B., Bernabé, R.M., Márquez, C., Gaffney, J.S., Marley, N.A., Laskin, A., Shutthanandan, V., Xie, Y., Brune, W., Lesher, R., Shirley, T., Jimenez, J.L., 2006. *Characterization of ambient aerosols in Mexico City during the MCMA-2003 campaign with Aerosol Mass Spectrometry: Results from the CENICA Supersite*. Atmos. Chem. Phys. 6, 925–946. https://doi.org/10.5194/acp-6-925-2006

Schober, P., Schwarte, L.A., 2018. *Correlation coefficients: Appropriate use and interpretation*. Anesth. Analg. 126, 1763–1768. https://doi.org/10.1213/ANE.0000000000002864

Shakya, K.M., Peltier, R.E., Shrestha, H., Byanju, R.M., 2017. *Measurements of TSP, PM_{10}, $PM_{2.5}$, BC, and PM chemical composition from an urban residential location in Nepal*. Atmos. Pollut. Res. 8, 1123–1131. https://doi.org/10.1016/j.apr.2017.05.002

Stavroulas, I., Grivas, G., Liakakou, E., Kalkavouras, P., Bougiatioti, A., Kaskaoutis, D.G., Lianou, M., Papoutsidaki, K., Tsagkaraki, M., Zarmpas, P., Gerasopoulos, E., Mihalopoulos, N., 2021. *Online Chemical Characterization and Sources of Submicron Aerosol in the Major Mediterranean Port City of Piraeus, Greece*. Atmosphere 12, 1686. https://doi.org/10.3390/atmos12121686

Sun, Y.L., Zhang, Q., Schwab, J.J., Demerjian, K.L., Chen, W.N., Bae, M.S., Hung, H.M., Hogrefe, O., Frank, B., Rattigan, O. V., Lin, Y.C., 2011. *Characterization of the sources and processes of organic and inorganic aerosols in New York city with a high-resolution time-of-flight aerosol mass spectrometer*. Atmos. Chem. Phys. 11, 1581–1602. https://doi.org/10.5194/acp-11-1581-2011

Talukdar, S., Tripathi, S.N., Lalchandani, V., Rupakheti, M., Bhowmik, H.S., Shukla, A.K., Murari, V., Sahu, R., Jain, V., Tripathi, N., Dave, J., Rastogi, N., Sahu, L., 2021. *Air pollution in new delhi during late winter: An overview of a group of campaign studies focusing on composition and sources*. Atmosphere (Basel). 12, 1–22. https://doi.org/10.3390/atmos12111432

Tõnisson, L., Kunz, Y., Kecorius, S., Madueño, L., Tamayo, E.G., Casanova, D.M., Zhao, Q., Schikowski, T., Hornidge, A.K., Wiedensohler, A., Macke, A., 2020. *From transfer to knowledge co-production: A transdisciplinary research approach to reduce black carbon emissions in metro manila, Philippines*. Sustain. 12, 1–19. https://doi.org/10.3390/su122310043

Ulevičius, V., Byčenkienė, S., Špirkauskaitė, N., Kecorius, S., 2010. *Biomass burning impact on black carbon aerosol mass concentration at a coastal site: Case studies*. Lithuanian J. Phys. 50, 335–344. https://doi.org/10.3952/lithjphys.50304

Tun, M.M., Juchelkova, D., Win, M.M., Thu, A.M., Puchor, T., 2019. *Biomass energy: An overview of biomass sources, energy potential, and management in Southeast Asian countries*. Resources 8. https://doi.org/10.3390/resources8020081

Ulevičius, V., Byčenkienė, S., Špirkauskaitė, N., Kecorius, S., 2010. *Biomass burning impact on black carbon aerosol mass concentration at a coastal site: Case studies*. Lithuanian J. Phys. 50, 335–344. https://doi.org/10.3952/lithjphys.50304

Virkkula, A., Mäkelä, T., Hillamo, R., Yli-Tuomi, T., Hirsikko, A., Hämeri, K., Koponen, I.K., 2007. *A Simple Procedure for Correcting Loading Effects of Aethalometer Data*. J. Air Waste Manag. Assoc. 57(10), 1214–1222. https://doi.org/10.3155/1047-3289.57.10.1214

Wang, J., Nie, W., Cheng, Y., Shen, Y., Chi, X., Wang, J., Huang, X., Xie, Y., Sun, P., Xu, Z., Qi, X., Su, H., Ding, A., 2018. *Light absorption of brown carbon in eastern China based on 3-year multi-wavelength aerosol optical property observations and an improved absorption Ångström exponent segregation method*. Atmos. Chem. Phys. 18, 9061–9074. https://doi.org/10.5194/acp-18-9061-2018

Wang, X., Heald, C.L., Sedlacek, A.J., de Sá, S.S., Martin, S.T., Alexander, M.L., Watson, T.B., Aiken, A.C., Springston, S.R., Artaxo, P. 2016. *Deriving brown carbon from multiwavelength absorption measurements: method and application to AERONET and Aethalometer observations*. Atmos. Chem. Phys. 16, 12733–12752. https://doi.org/10.5194/acp-16-12733-2016

Weingartner, E., Saathoff, H., Schnaiter, M., Streit, N., Bitnar, B., Baltensperger, U., 2003. *Absorption of light by soot particles: Determination of the absorption coefficient by means of aethalometers*. J. Aerosol Sci. 34, 1445–1463. https://doi.org/10.1016/S0021-8502(03)00359-8

Werden, B.S., Giordano, M.R., Goetz, J.D., Islam, M.R., Bhave, P. V., Puppala, S.P., Rupakheti, M., Saikawa, E., Panday, A.K., Yokelson, R.J., Stone, E.A., DeCarlo, P.F., 2022. *Premonsoon submicron aerosol composition and source contribution in the Kathmandu Valley, Nepal*. Environ. Sci. Atmos. 2, 978–999. https://doi.org/10.1039/d2ea00008c

WHO, 2021. *WHO global air quality guidelines*. Coast. Estuar. Process. 2021, 1–360.

Williams, L., Aerodyne Team, 2021. *AMS/ACSM Calibration Protocols*. ARI AMS Users Meeting, Virtual, January 19, 2021.

Wmo/Igac, 2012. *Impacts of Megacities on Air Pollution and Climate*, Global Atmosphere Watch (GAW) Rep.

No. 205., WMO/IGAC.

Xie, C., Xu, W., Wang, J., Wang, Q., Liu, D., Tang, G., Chen, P., Du, W., Zhao, J., Zhang, Y., Zhou, W., Han, T., Bian, Q., Li, J., Fu, P., Wang, Z., Ge, X., Allan, J., Coe, H., Sun, Y., 2019. *Vertical characterization of aerosol optical properties and brown carbon in winter in urban Beijing*. Atmos. Chem. Phys. 19, 165–179. https://doi.org/10.5194/acp-19-165-2019

Yang, M., Howell, S.G., Zhuang, J., Huebert, B.J., 2009. *Attribution of aerosol light absorption to black carbon, brown carbon, and dust in China*. Atmos. Chem. Phys. 9, 2035–2050. https://doi.org/10.5194/acp-9-2035-2009

Yu, J., Zhu, A., Liu, M., Dong, J., Chen, R., Tian, T., Liu, T., Ma, L., Ruan, Y., 2023. *Association between air pollution and cardiovascular disease hospitalizations in Lanzhou City, 2013–2020: A time series analysis*. GeoHealth 8, e2022GH000780. https://doi.org/10.1029/2022GH000780

Zhou, S., Collier, S., Jaffe, D.A., Briggs, N.L., Hee, J., Iii, A.J.S., Kleinman, L., Onasch, T.B., Zhang, Q., 2017. *Regional influence of wildfires on aerosol chemistry in the western US and insights into atmospheric aging of biomass burning organic aerosol*. Atmos. Chem. Phys. 17, 2477–2493. https://doi.org/10.5194/acp-17-2477-2017

Zhang, Y., Albinet, A., Petit, J.E., Jacob, V., Chevrier, F., Gille, G., Pontet, S., Chretien, E., Dominik-Segue, M., Levigoureux, G., Mocnik, G., Gros, V., Jaffrezo, J.L., Favez, O., 2020. *Substantial brown carbon emissions from wintertime residential wood burning over France*. Sci. Total Environ. 743, 140752. https://doi.org/10.1016/j.scitotenv.2020.140752

Zhao, Z., Cao, J., Chow, J.C., Watson, J.G., Chen, L.-W., Wang, X., Wang, Q., Tian, J., Shen, Z., Zhu, C., Liu, S., Tao, J., Ye, Z., Zhang, T., Zhou, J., 2019. *Multi-wavelength light absorption of black and brown carbon at a high-altitude site on the Southeastern margin of the Tibetan Plateau, China*. Atmos. Environ. 212, 54–64. https://doi.org/10.1016/j.atmosenv.2019.05.035

Zuo, P., Huang, Y., Bi, J., Wang, W., Li, W., Lu, D., Zhang, Q., Liu, Q., Jiang, G., 2023. *Non-traditional stable isotopic analysis for source tracing of atmospheric particulate matter*. Trend. Anal. Chem. 158, 116866. https://doi.org/10.1016/j.trac.2022.116866

Zotter, P., Herich, H., Gysel, M., El-Haddad, I., Zhang, Y., Mocnik, G., Hüglin, C., Baltensperger, U., Szidat, S., Prévôt, A.S.H., 2017. *Evaluation of the absorption Ångström exponents for traffic and wood burning in the Aethalometer-based source apportionment using radiocarbon measurements of ambient aerosol*. Atmos. Chem. Phys. 17, 4229–4249. https://doi.org/10.5194/acp-17-4229-2017